The molecular basis for functional divergence of duplicated SOX factors controlling endoderm formation and left-right patterning in zebrafish

Simaran Johal[1,2], Randa Elsayed[3], Kristen A. Panfilio[1,4,5], Andrew C. Nelson[1*]

1. School of Life Sciences, Gibbet Hill Campus, University of Warwick, Coventry, CV4 7AL, UK

2. Current address: Translational and Clinical Research Institute, Herschel Building, Newcastle University, Newcastle Upon Tyne, NE1 7RU, UK

3. Warwick Medical School, Gibbet Hill Campus, University of Warwick, Coventry, CV4 7AL, UK

4. Department of Molecular Genetics, Institute of Biology, University of Hohenheim, Garbenstr. 30, 70599 Stuttgart, Germany

5. Institute for Zoology: Developmental Biology, University of Cologne, Zülpicher Straße 47b, 50674 Cologne, Germany

*Corresponding author
Email: A.Nelson.1@warwick.ac.uk (ACN)

Abstract

Endoderm, one of three primary germ layers of vertebrate embryos, makes major contributions to the respiratory and gastrointestinal tracts and associated organs, including liver and pancreas. In mammals, the transcription factor *SOX17* is vital for endoderm organ formation and can induce endoderm progenitor identity. Duplication of ancestral *sox17* in the teleost lineage produced the paralogues *sox32* and *sox17* in zebrafish. Sox32 is required for specification of endoderm and progenitors of the left-right organiser (Kupffer's Vesicle, KV), with Sox17 a downstream target of Sox32 that is implicated in further KV development. Phenotypic evidence therefore suggests functional similarities between zebrafish Sox32 and Sox17 and mammalian SOX17. Here, we directly compare these orthologues and paralogues, using the early zebrafish embryo as a biological platform for functional testing. Our results indicate that, unlike Sox32, human SOX17 cannot induce endoderm specification in zebrafish. Furthermore, using hybrid protein functional analyses, we show that Sox32 specificity for the endoderm gene regulatory network is linked to evolutionary divergence in its DNA-binding HMG domain from its paralogue Sox17. Additionally, changes in the C-terminal regions of Sox32 and Sox17 underpin their differing target specificities. Finally, we establish that specific conserved peptides in the C-terminal domain are essential for the role of Sox17 in establishing correct organ asymmetry. Overall, our results illuminate the molecular basis for functional divergence of Sox32 and Sox17 in vertebrate endoderm development and left-right patterning, and the evolution of SoxF transcription factor function.

Introduction

Sox family transcription factors (TFs) are evolutionarily conserved proteins with roles in cell fate decisions in a range of developmental processes (Sarkar and Hochedlinger 2013). Mutations in Sox factors have been linked to an array of developmental defects and congenital diseases in humans (Angelozzi and Lefebvre 2019). Sox TFs belong to the superfamily of High Mobility Group (HMG) domain containing TFs. Historically, membership of the Sox family has been dictated by having >50% conservation of the DNA-binding HMG domain with mouse SRY – the founding Sox TF (Gubbay, et al. 1990; Sinclair, et al. 1990; Pevny and Lovell-Badge 1997). Sox factors have been further characterised into subfamilies, whereby members of a subfamily exhibit 75-80% homology within their HMG domain (Bowles, et al. 2000; Wegner 2010). One subfamily is SoxF, which in mammals consists of SOX7, SOX17 and SOX18. In teleosts, SoxF is expanded to include Sox32. How has this additional TF been functionally integrated into SoxF developmental gene regulatory networks (GRNs)?

Most duplicated *sox* genes in the teleost lineage arose through a whole genome duplication event that occurred 226-316 million years ago (Voldoire, et al. 2017). An exception to this is *sox32,* which is hypothesised to have emerged through tandem duplication of *Sox17* (Voldoire, et al. 2017). While we and others have speculated that zebrafish Sox32 may function in similar processes to mammalian SOX17 (Lilly, et al. 2017; Figiel, et al. 2021), this has not been explored at the molecular level. Furthermore, it is unknown whether functions of the ancestral gene have been split among the two paralogues (sub-functionalisation) or whether they have functionally diverged post-duplication and acquired new roles (neo-functionalisation).

Sox32 is considered the master-regulator of endoderm identity in zebrafish. Loss-of-function mutations in *sox32* lead to a profound loss of endoderm progenitors and consequent absence of the respiratory tract and gut, and its associated organs including the liver and pancreas. Instead, presumptive endoderm cells differentiate into mesoderm (Alexander, et al. 1999; Dickmeis, et al. 2001). Conversely, *sox32* overexpression (OE) through mRNA injection during early development is sufficient to respecify presumptive mesodermal cells to endodermal fates, resulting in ectopic endoderm formation (Kikuchi, et al. 2001). Furthermore, transplantation studies show that cells from *sox32* mRNA-injected donor zebrafish embryos preferentially incorporate into developing endoderm tissues in wild type hosts, and they are capable

of endoderm restoration in Sox32-deficient hosts (Kikuchi, et al. 2001; Aoki, et al. 2002; Stafford, et al. 2006).

Similarly, *Sox17* null mutant mice are embryonic lethal and show narrower expression domains of definitive endoderm markers in the embryonic gut, indicating that loss of Sox17 results in depletion of the definitive endoderm (Kanai-Azuma, et al. 2002). Furthermore, ectopic expression of SOX17 in mouse and human embryonic stem cells (ESCs) causes differentiation towards the extraembryonic and definitive endoderm fates, respectively (Séguin, et al. 2008; Niakan , et al. 2010; McDonald, et al. 2014). Thus, phenotypic evidence suggests functional similarity between SoxF subfamily members, with both mammalian SOX17 and zebrafish Sox32 inducing endoderm cell identity within their respective species. However, a molecular functional comparison is lacking.

In zebrafish, Sox32 is also required for correct specification of the Dorsal Forerunner Cells (DFCs) – progenitors of the left-right (LR) organiser, which is essential for correct positioning of endoderm-derived organs within the body cavity (Alexander, et al. 1999; Essner, et al. 2005). Specifically, the DFCs give rise to the zebrafish laterality organ, known as Kupffer's Vesicle (KV) (Cooper and D'Amico 1996; Melby, et al. 1996; Essner, et al. 2005; Warga and Kane 2018). KV function involves cilia-mediated fluid flow in an anti-clockwise direction, which leads to unilateral induction in the left lateral plate mesoderm (LPM) of Nodal (Spaw in teleosts, (Long, et al. 2003; Montague, et al. 2018)). Defects in KV formation and cilia function lead to abnormalities in Nodal expression and consequent laterality defects affecting organs including the brain, heart, and pancreas (Essner, et al. 2005; Kramer-Zucker, et al. 2005). As a downstream target of its paralogue Sox32, Sox17 is implicated in KV function (Aamar and Dawid 2010). Similarly, in mice Sox17 is implicated in the establishment of LR patterning, both indirectly through an inability to maintain gut endoderm in *Sox17*$^{-/-}$ mutants, and directly through defects in the morphogenesis of the mouse laterality organ (the node) (Kanai-Azuma, et al. 2002; Saund, et al. 2012). An outstanding question is which regions of the Sox17 protein mediate key functions in establishment of LR asymmetry and consequent organ patterning and placement.

Building on previous phenotypic observations, and to gain novel insights at the molecular level, here we examine whether SoxF factors exhibit functional conservation across species and identify functional domains within the zebrafish Sox32 and Sox17 proteins that are required for their respective developmental roles in endoderm

117 specification and LR patterning. We performed molecular dissection and hybrid protein
118 functional analyses of zebrafish Sox32 and Sox17 to draw functional comparisons with
119 human SOX17 (hSOX17). We find that Sox32 shares limited functional similarities with
120 hSOX17 or Sox17, with neither of the latter two able to induce endoderm specification
121 in the zebrafish embryo. Sox17 and hSOX17 also differ from each other in terms of
122 molecular capabilities. In detail, Sox32's fundamental role in initiating the zebrafish
123 endoderm GRN appears to be linked to evolutionary divergence in its HMG domain.
124 We also show how changes in putative helical peptides within their C-terminal domains
125 (CTDs) account for the zebrafish paralogues' differing functional roles, including in cell
126 fate specification and organ placement. Overall, our analyses reveal how divergence
127 in specific protein domains underpins distinct TF target gene repertoires. We thus
128 elucidate the SoxF molecular evolutionary changes that determine endoderm GRN
129 specificity in the teleost and mammalian lineages.
130

131 **Results**

132 **hSOX17 cannot induce endoderm identity in zebrafish embryos**

133 Although hSOX17 and Sox32 can induce endoderm in humans and zebrafish,
134 respectively, these orthologues' molecular capabilities have not been tested in a
135 directly comparable biological context. Also, it is unknown whether Sox17, downstream
136 of Sox32, can induce endoderm gene expression directly. To address this, we injected
137 equimolar quantities of mRNA encoding hSOX17, Sox32 or Sox17 into the zebrafish
138 embryo at the one-cell stage, followed by RNA-seq analysis at 6 hours post-fertilisation
139 (hpf), the stage by which endoderm has been specified in wild type embryos (Figure
140 1A).

141 Sox32 overexpression (OE) elicited widespread changes in gene expression
142 compared to Sox17, with hSOX17 affecting relatively few genes (Figure 1B-C,
143 Supplementary Figure S1, Supplementary Tables S1-5). We observed a small but
144 significant overlap in upregulated transcripts between Sox32 and hSOX17, and Sox32
145 and Sox17, but not between hSOX17 and Sox17 (Figure 1C-F). Thus, Sox32 appears
146 functionally more similar to both hSOX17 and Sox17 than hSOX17 and Sox17 are to
147 each other in the context of the early zebrafish embryo. Overall, this suggests key

148 differences in the functional capabilities of these three Sox factors.

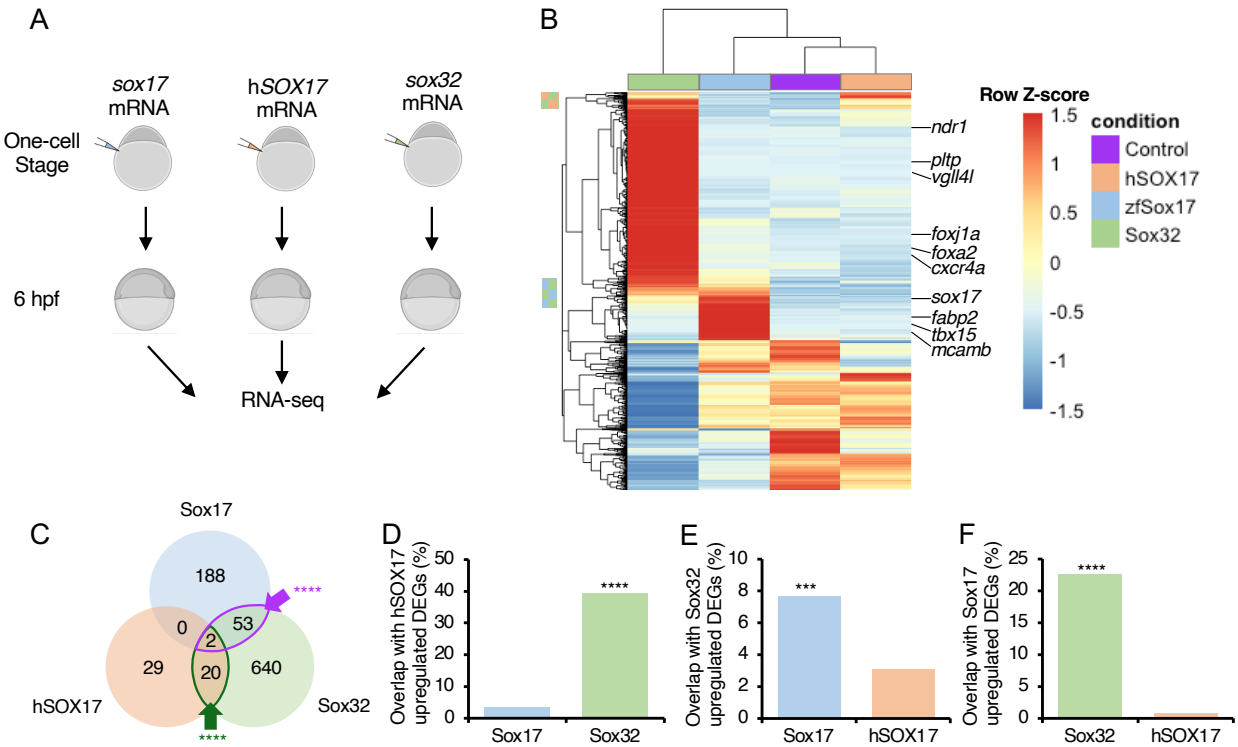

Figure 1: Sox32, Sox17 and hSOX17 are capable of inducing largely distinct gene sets in the early zebrafish embryo. A) Experimental schematic. **B)** Heatmap of all 1628 differentially expressed genes (DEGs, Supplementary Table S1-3), displayed as median counts from N=3 per condition. Colour-coded blocks to the left indicate genes induced by both hSOX17 and Sox32, and by Sox17 and Sox32. **C)** Venn diagram showing overlap of genes (Supplementary Table S4) significantly upregulated by each TF ($P < 0.05$). Overlaps significantly greater than expected according to Fisher's Exact test are indicated. **** $P < 0.0001$. **D-F)** Bar charts indicating percentage overlap of upregulated DEGs to (D) hSOX17, (E) Sox32, and (F) Sox17 upregulated DEGs. Bars represent the percentage of genes upregulated by the factor on the y-axis also upregulated by the factor on the x-axis; note the TF-specific y-axis scale for each chart. Statistical tests to determine whether the overlap was significantly greater with one factor on the x-axis compared to the other were carried out using Fisher's Exact test. *** $P<0.001$, **** $P <0.0001$.

149 To examine the pathways and processes influenced by OE of these TFs, we
150 performed functional and anatomical annotation analysis of the differentially expressed
151 genes (DEGs), including comparison to established cell identity markers from single-
152 cell (sc)RNA-seq time course analysis of the early embryo (Wagner, et al. 2018). This
153 revealed largely distinct results for each TF, further supporting the notion that they are
154 functionally distinct in this context (Supplementary Figure S2-S3). As expected,
155 transcripts upregulated by Sox32 OE were significantly enriched for terms associated
156 with endoderm development (Supplementary Figure S3). This includes 6 hpf
157 "nondorsal involuted anterior", which contains endoderm progenitors, and 8 hpf
158 endoderm. Transcripts induced by Sox32 also showed strong enrichment for 8 hpf
159 DFC markers, suggesting that Sox32 is not only necessary (Alexander, et al. 1999) but

also sufficient to drive DFC gene expression. In comparison, Sox17 OE results in a less profound effect on endoderm marker expression, with no significant effect on 6 hpf nondorsal involuted anterior marker induction but modest significant enrichment for endoderm makers at 8 hpf and for DFC markers, consistent with a role in KV formation and function (Supplementary Figure S3). Meanwhile, genes upregulated after hSOX17 ectopic expression did not yield any significantly enriched gene ontology terms, and downregulated genes do not pertain to endoderm but may be indicative of mis-regulation of Wnt signalling (Supplementary Figure S2).

Beyond endoderm development, analysis of transcripts upregulated by Sox17 revealed significant enrichment for terms associated with cardiovascular development, such as “Regulation of Sprouting Angiogenesis”, “Endothelial Tube Morphogenesis” and “Endocardium” (Supplementary Figure S2). This is consistent with *sox17* expression patterns during cardiovascular development in both zebrafish and mammals (Chung, et al. 2011; Saba, et al. 2019) (Supplementary Figure S4, Supplementary Video S1), and known *Sox17* loss-of-function phenotypes in mice vasculature and heart (Kanai-Azuma, et al. 2002; Saba, et al. 2019).

Thus, functional and anatomical enrichment analyses suggest Sox17 has different roles in early developmental processes compared to its paralogue Sox32, and hSOX17 cannot induce endoderm specification in zebrafish.

Sox32 has a divergent HMG domain and longer C-terminal helix

To determine which structural motifs may explain the functional differences between Sox32, Sox17 and hSOX17, we analysed AlphaFold structural predictions and performed protein sequence alignments (Figure 2A-E). 3D structural models indicate a very high confidence prediction in the centre of all three proteins corresponding to the HMG domain. The HMG domains of Sox17 and hSOX17 are most similar, with 92% amino acid identity, while the Sox32 HMG domain differs from both Sox17 and hSOX17 with 67% and 69% identity, respectively (Figure 2D). Interestingly, 44% of amino acid differences between Sox32 and Sox17 correspond to changes in chemical properties that may influence the 3D folding of the protein, resulting in exposure of different residues to binding partners.

192 Another notable structured region within Sox32 is a predicted 25-aa C-terminal
193 helix (Figure 2A). C-terminal helices were also predicted in Sox17 (Figure 2B) and
194 hSOX17 (Figure 2C), albeit the confidence of the prediction is lower and they are
195 shorter (Figure 2E). Amino acid sequence alignments of the putative helices suggest
196 the overall level of conservation is low, although they do encompass a seven amino
197 acid peptide region previously recognised to be conserved throughout the SoxF
198 subfamily, including in Sox7 and Sox18 (Kikuchi, et al. 2001; Sinner, et al. 2004)
199 (Supplementary Figure S5). This 7-aa Sox32 peptide (EFDQYLN, Figure 2E) has
200 previously been shown to be required for Sox32 induction of endoderm fate (Zhao, et
201 al. 2013).

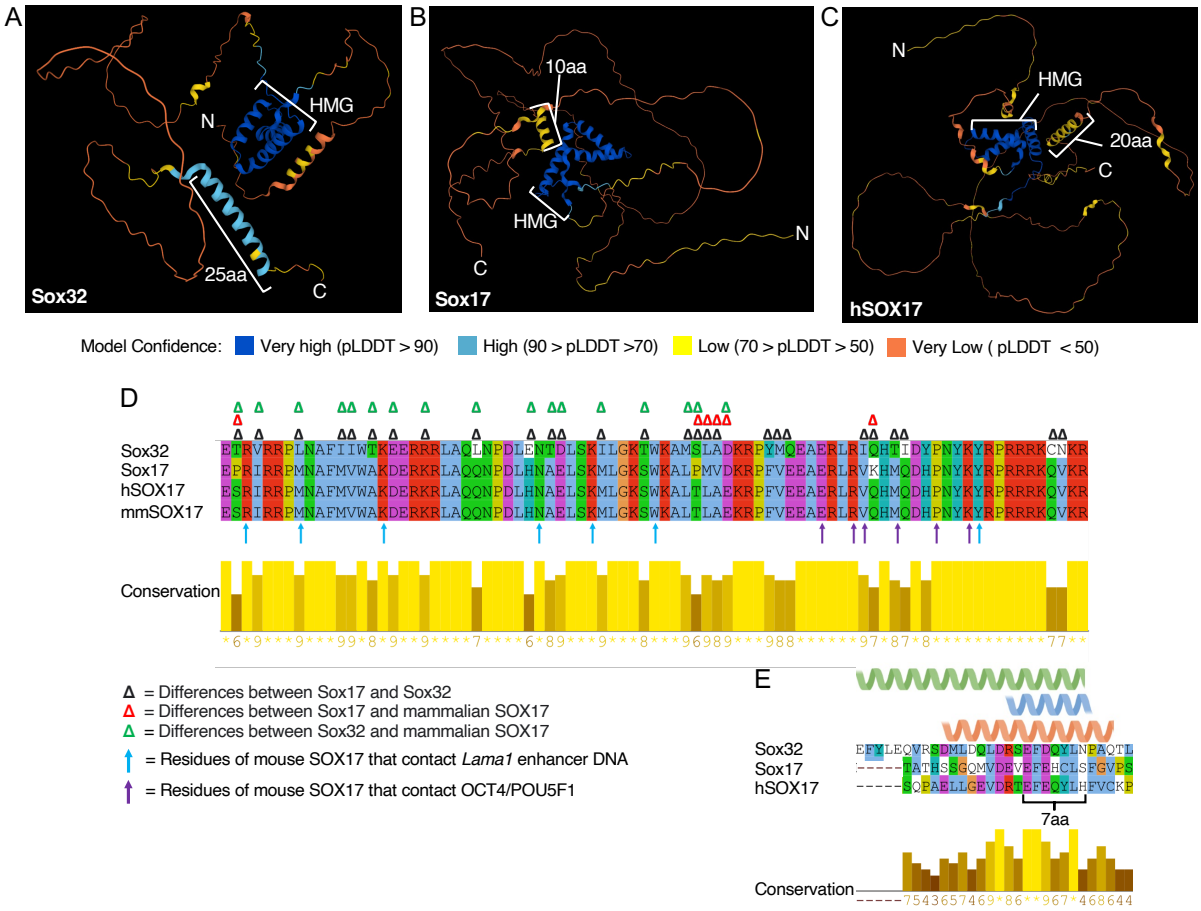

Figure 2: AlphaFold predicts C-terminal helical domains within Sox32, Sox17 and hSOX17. A-C) Alphafold models coloured by model confidence as shown in the key. DNA-binding HMG domains and C-terminal helices of different lengths are annotated. **(D)** Alignment of HMG domains of Sox32, Sox17, hSOX17 and *Mus musculus* (mm)Sox17. Alignment was carried out using Clustal Omega in Jalview, and colour coded based on conserved amino acid properties. Conservation levels calculated according to Analysis of Multiply Aligned Sequences (AMAS) displayed. Delta symbols denote differences in amino acids as per the key. Arrows indicating mapped amino acid contact sites between mouse SOX17 and the *Lama1* enhancer (Blue), and equivalent SOX2 sites and OCT4/POU5F1 protein (Purple). (Palasingam, et al. 2009; Ng, et al. 2012) . **(E)** Alignment of CTD helical domain region for Sox32, Sox17 and hSOX17. Amino acids within Alphafold predicted helical domains annotated: Green = Sox32; blue = Sox17; peach = hSOX17. The 7-aa peptide previously shown to be required for Sox32 induction of endoderm fate (Zhao, et al. 2013) is also annotated.

202 Overall, we conclude that the Sox32 HMG domain shows a higher degree of
203 divergence from the common ancestor than Sox17 or hSOX17. Additionally, we identify
204 putative CTD helices of differing lengths between these Sox factors that encompass a
205 7-aa peptide region of known importance in Sox32.
206
207 **Sox32 specificity for the endoderm GRN is driven by HMG domain divergence**
208 Compared to its homologues, Sox32 has a unique property allowing it to induce
209 the zebrafish endoderm GRN (Figure 1), and divergence in the DNA-binding HMG
210 domain (Figure 2D) may confer this function. To examine this, we tested the ability of
211 a hybrid protein (HMG Switch), consisting of the Sox32 N- and CTDs flanking the
212 Sox17 HMG domain, to induce endoderm gene expression, compared to wild type
213 Sox32 and Sox17 proteins and a Sox32 protein lacking the HMG domain
214 (Sox32ΔHMG, Figure 3A). These proteins' transcriptional effects were assayed by
215 RNA-seq after early ectopic mRNA injection (Figure 3B).
216 As expected in the absence of a DNA-binding domain, Sox32ΔHMG failed to
217 induce Sox32 target genes (Figure 3B). In contrast, HMG Switch-induced genes show
218 significant overlap with both Sox32- and Sox17-induced genes, with either paralogue's
219 HMG domain sufficient for the induction of a core set of 180 target genes (Figure 3C).
220 This is further supported in pairwise comparisons (Figure 3D-F). In fact, the majority of
221 Sox17-induced genes are also induced by the HMG Switch protein (Figure 3C: 152 of
222 194 DEGs), underscoring the importance of the HMG domain for specific induction of
223 Sox17 targets. However, the HMG Switch protein has a distinct TF profile, with over
224 half (58.8%) of its target genes not induced by either Sox32 or Sox17. Furthermore,
225 58.9% of Sox32-induced genes are not induced by HMG Switch (Figure 3C). Taken
226 together, this indicates that amino acid differences distinguishing the Sox32 and Sox17
227 HMG domains confer significant functional differences.
228 Functional annotation of induced target genes further illustrates the limits of the HMG
229 Switch protein to recapitulate Sox32's induction of specific cell identities (Figure 3G).
230 Sox32 has a stronger capacity to significantly induce markers of endoderm and DFC
231 cell types than the HMG Switch, and this enrichment occurs at the expense of other
232 cell types such as the adaxial mesoderm and ventral ectoderm. This suggests the
233 Sox32 HMG domain shows endodermal target specificity and is required to induce cell
234 fate changes. Furthermore, while HMG Switch provides significant induction of

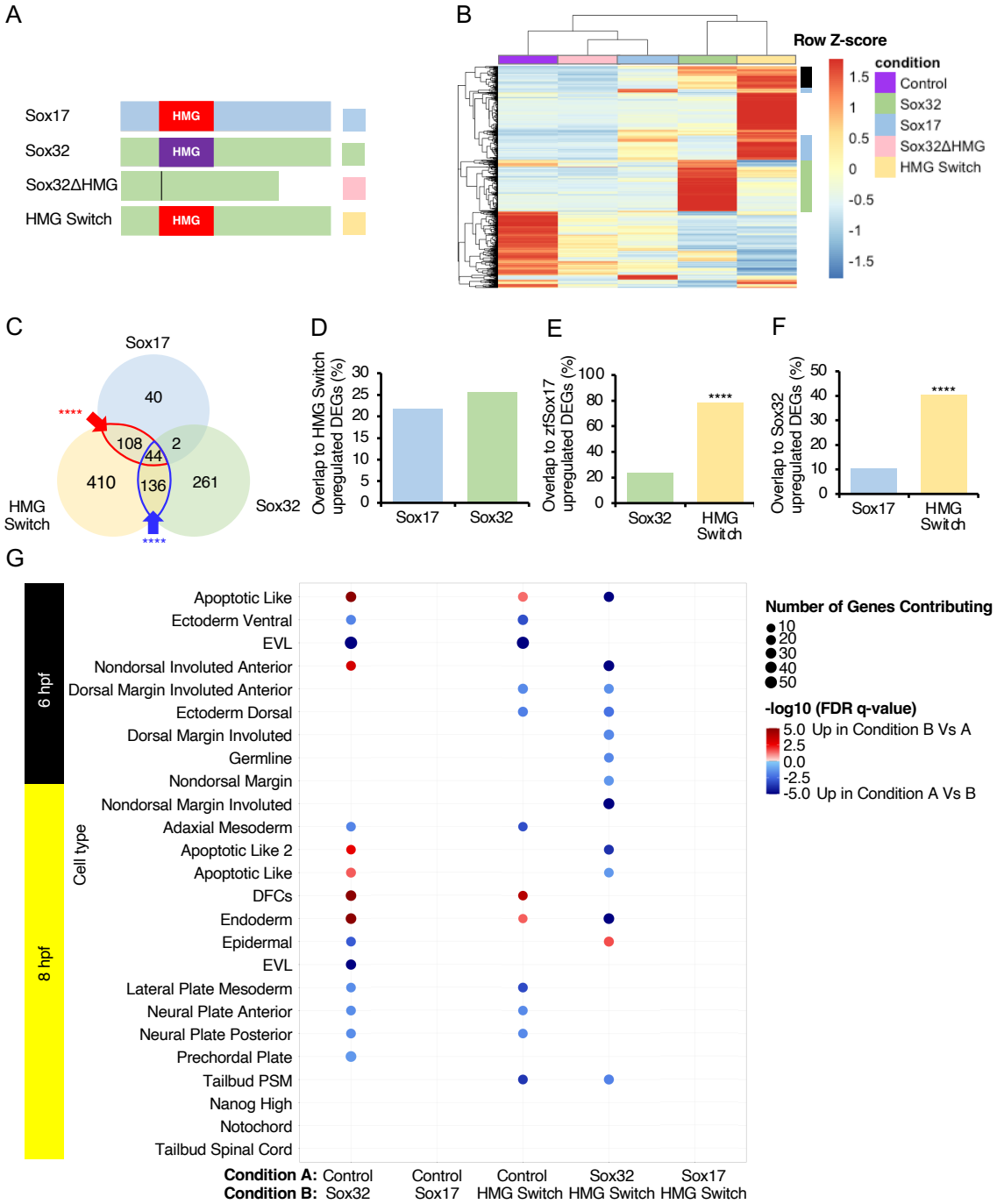

Figure 3: Differences between the Sox32 and Sox17 HMG domains are critical to the ability of Sox32 to induce endoderm and DFC gene expression. A) Protein models depicting constructs injected at the one-cell stage followed by RNA-sequencing at 6 hpf. **B)** Heatmap of all 1572 DEGs (Supplementary Tables S6-10), depicted as median counts from N=2 per condition. Green sidebar: induction of genes requiring the Sox32 HMG domain. Blue sidebar: induction of genes requiring the Sox17 HMG domain. Black sidebar: genes induced by Sox32 with either Sox32 or Sox17 HMG domain. **C)** Overlap of upregulated DEGs. Overlaps greater than expected according to Fisher's Exact test are indicated - **** P < 0.0001. **D-F)** Percentage overlap of upregulated DEGs to (D) HMG Switch, (E) Sox17, (F) Sox32 upregulated DEGs. Bars represent the percentage of genes upregulated by the factor on the y-axis also upregulated by the factor on the x-axis. Statistical tests to determine whether the overlap was significantly greater with one factor on the x-axis compared to the other were carried out using Fisher's Exact test.. **** P < 0.001. **G)** Gene Set Enrichment Analysis (GSEA) carried out against cell type markers defined by scRNA-seq at 6 and 8 hpf (Wagner, et al. 2018). EVL - enveloping layer; DFCs – dorsal forerunner cells; PSM – presomitic mesoderm.

235 endoderm markers compared to the control, Sox32 exhibits significantly greater

236 induction of endoderm markers compared to HMG Switch (Figure 3G).

237 Overall, we conclude that the divergence of the Sox32 HMG domain from
238 ancestral Sox17 is critical in conferring endoderm and DFC target specificity within the
239 zebrafish embryo.

240

241 **The Sox32 25-aa C-terminal helix is required for induction of endoderm and DFC**
242 **marker genes while the NTD has target-specific functions**

243 Beyond the HMG domain, we also find evidence that the flanking protein regions
244 influence target gene induction. One-fifth of Sox17's targets are unique (Figure 3C),
245 implicating other domains in determining the full repertoire of TF-specific target genes.
246 This is further corroborated by the sizable overlap in induced targets between the HMG
247 Switch and Sox32 proteins despite differing HMG domains (Figure 3C: 136 targets).
248 We therefore next explored which peptides outside the Sox32 HMG domain are
249 required for target gene induction.

250 The Sox32 N-terminal domain (NTD) contains a conserved EKR
251 phosphorylation motif that, when phosphorylated in response to FGF signalling, leads
252 to attenuation of Sox32 function, antagonising endoderm specification (Poulain 2006).
253 Furthermore, examination of conservation across *sox32* orthologues revealed
254 conservation of a 30-aa region within the Sox32 CTD, which we consider in two parts.
255 Specifically, previous studies have identified a 7-aa β-catenin interacting peptide, with
256 higher conservation between Sox32 and hSOX17 than Sox17 (Kikuchi, et al. 2001;
257 Sinner, et al. 2004), that is required for Sox32 induction of ectopic endoderm upon OE
258 (Zhao, et al. 2013). An upstream 23-aa peptide conserved among *sox32* orthologues
259 remains unstudied (Supplementary Figure S5). Furthermore, AlphaFold predicts a high
260 confidence 25-aa long CTD helix which partly encompasses these two peptide regions
261 (Figure 2).

262 To examine the importance of these identified peptides to Sox32 target
263 induction, we carried out specific domain deletions. We then analysed the ability of
264 these domain-deleted mRNAs injected at the one-cell stage to induce five diagnostic
265 endoderm and DFC cell marker genes relative to full length (FL)-Sox32 by 6 hpf (Figure
266 4A). All selected markers show induction by FL-Sox32 in RNA-seq experiments (Figure
267 1B), with tissue-specific expression in the endoderm only (*foxa2*) (Alexander, et al.
268 1999), endoderm and DFCs (*sox17, cxcr4a*) (Kikuchi, et al. 2000; Thisse 2001) or
269 DFCs only (*vgll4l, ndr1*) (Rebagliati, et al. 1998; Thisse 2001).

270 Consistent with our global RNA-seq profiling (Figure 3B), Sox32 can strongly
271 induce all marker genes and the HMG domain is essential (Figure 4B-F: FL-Sox32 and
272 Sox32ΔHMG constructs). Equally, both peptides within the CTD helix are required, as
273 Sox32Δ7aa and Sox32Δ23aa OE show no deviation in expression of target genes
274 compared to control embryos (Figure 4B-F), except for significant induction of *cxcr4a*
275 still attained with the Sox32Δ7aa construct.

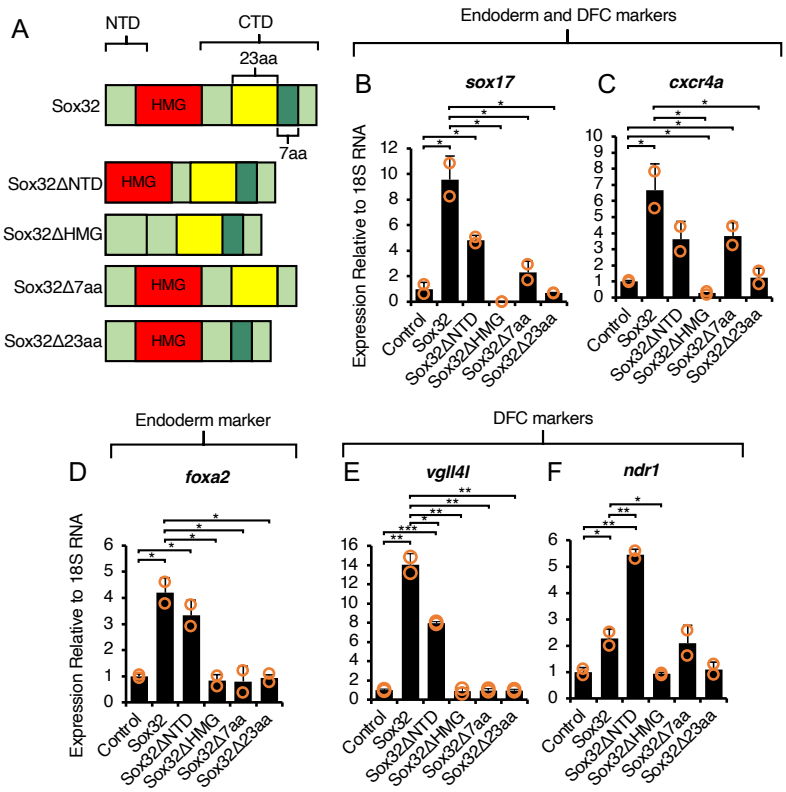

Figure 4: Putative helical CTD peptides highly conserved between Sox32 orthologues are required for induction of downstream endoderm and DFC marker genes, while NTD function is target-specific. A) Protein models of Sox32 deletions injected at the one-cell stage and RNA extraction followed by qPCR at 6 hpf. **B-F)** qPCR analysis of endoderm and DFC (B,C) endoderm only (D), and DFC only (E-F) markers. Bar charts depict the mean fold change relative to uninjected controls, error bars ± one standard deviation, orange circles indicate individual datapoints. Statistical tests on biological duplicate samples were carried out using Student's *t*-test. * P<0.05, ** P <0.01, *** P<0.001.

276 The role of the NTD appears more complex, with differing roles depending on
277 the target gene. Overall, the NTD would seem dispensable, as Sox32ΔNTD can
278 significantly induce all analysed genes compared to the control, and with comparable
279 levels of expression of the endoderm-only marker *foxa2* (Figure 4B). However, the
280 Sox32ΔNTD construct only induced the dual endoderm/DFC markers *sox17* and
281 *cxcr4a* to about half the level of FL-Sox32 (Figure 4C-D). Furthermore, for DFC-
282 specific marker genes, relative induction by FL-Sox32 and Sox32ΔNTD differed, with
283 significantly greater induction of *vgll4l* with the full-length protein but, conversely,

284 significantly higher *ndr1* levels with the NTD-deleted construct (Figure 4E-F). Thus, the
285 NTD may offer a tuneable interface for context-specific target gene regulation by
286 Sox32, with the DFCs potentially evincing subtle modulation for different marker genes.
287

288 **Divergence of C-terminal peptides confers Sox32 and Sox17 differential target**
289 **specificity**

290 Sox32 requires its CTD helix for proper induction of its endodermal and DFC
291 targets, specifically the 7-aa peptide (Figure 4), which is also necessary to induce
292 ectopic endoderm upon Sox32 OE (Zhao, et al. 2013). This 7-aa region shows
293 complete conservation to the zebrafish SoxF subfamily members Sox7 and Sox18
294 (Supplementary Figure S5) and high conservation to hSOX17. However, the 7-aa
295 peptide is divergent in Sox17 (Figure 5A). This poses a question of whether this
296 divergence between Sox32 and Sox17 confers differential target specificity. To
297 decipher this, we generated constructs in which the respective 7-aa CTD regions were
298 deleted from both Sox32 and Sox17, and hybrid constructs were also generated with
299 7-aa peptides switched between the two TFs (Figure 5B). Lastly, as the overall C-
300 terminal helix structure also differs between Sox32 and Sox17 (Figure 2), we also
301 produced a construct with the longer 25-aa Sox32 CTD helical peptide replacing the
302 Sox17 7-aa peptide (Figure 5B).

303 Based on injections of each of the resulting mRNAs at the one-cell stage and
304 qPCR analysis of target genes that distinguish Sox32 and Sox17 (Figure 1B), we find
305 that induction of Sox17 targets indeed requires the Sox17 7-aa peptide. Replacement
306 with the Sox32 7-aa fails to elicit FL-Sox17 levels of induction (Figure 5C-E). The
307 replacement of the Sox17 7-aa peptide with the Sox32 25-aa peptide does not allow
308 Sox17 to induce Sox32 targets (Figure 5G-H). Therefore, while the Sox32 CTD helix
309 is necessary for Sox32 induction of endoderm and DFC targets (Figure 4), it is not
310 sufficient in the context of the Sox17 protein. However, replacement of the Sox17 7-aa
311 peptide with the Sox32 25-aa peptide does result in significant induction of Sox17
312 targets *fabp2* and *mcamb* compared to the control (Figure 5D-E). We therefore
313 conclude that the Sox32 25-aa peptide that makes up the Sox32 CTD helix appears to
314 be a potent transactivation domain.

315 In addition to replacement of the Sox17 7-aa peptide with that of Sox32 not
316 inducing Sox17 targets to the capacity of FL-Sox17 (Figure 5C-E), we also see that
317 replacement of the Sox32 7-aa peptide with the Sox17 7-aa peptide cannot induce

318 *foxj1a* or *vgll4l* to the same level as FL-Sox32 (Figure 5G). This indicates that both
319 Sox32 and Sox17 require their own intrinsic 7-aa domain for efficient induction of their
320 respective targets. Therefore, we suggest that divergence in C-terminal peptides

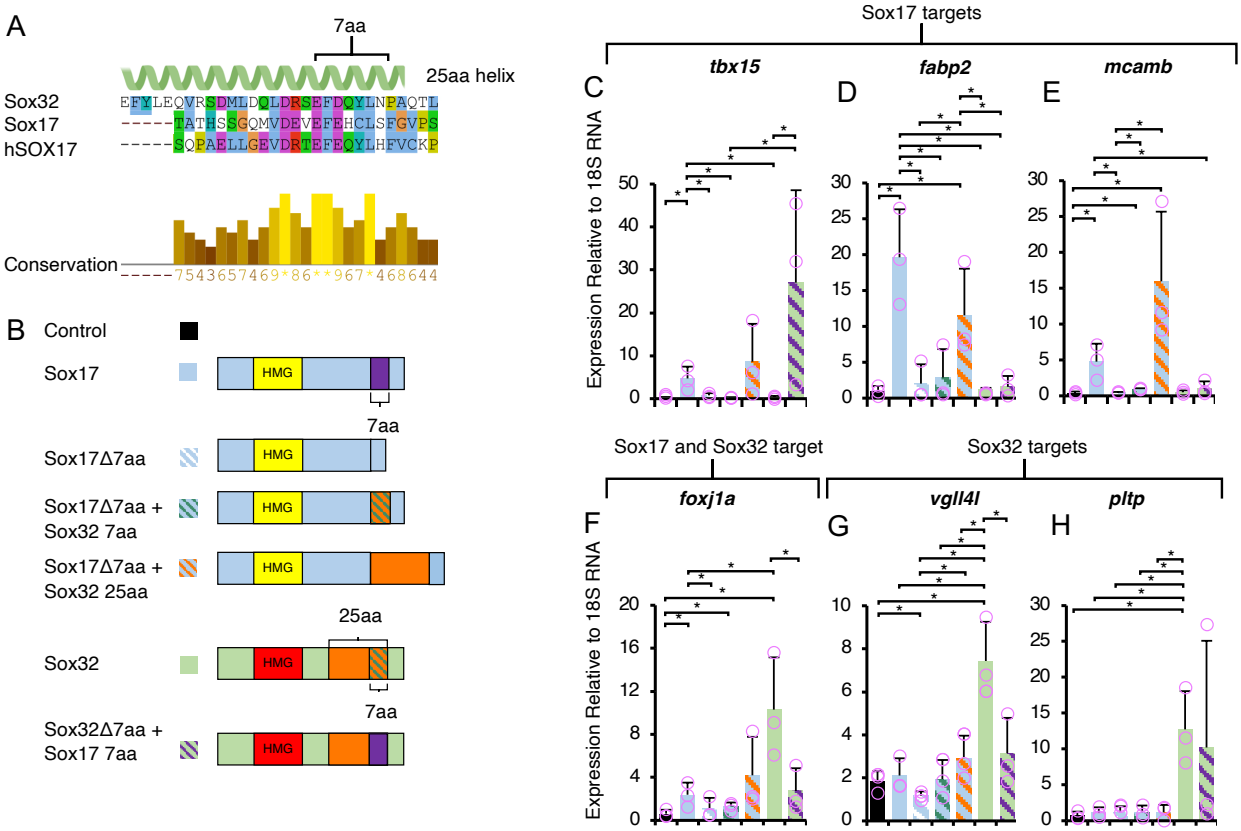

Figure 5: Divergence of 7-aa CTD putative helical peptides confers differential target specificity of Sox32 and Sox17. A) Alignment of Sox32 CTD helix (25 aa) to Sox17 and hSOX17 with conservation indicated. Alignment carried out using Clustal Omega in Jalview and colour coded based on conserved amino acid properties. Conservation levels calculated according to Analysis of Multiply Aligned Sequences (AMAS) displayed. **B)** Protein models of Sox17 and Sox32 domain deletions and switches injected at the one-cell stage and RNA extraction followed by qPCR at 6 hpf. **C-H)** qPCR of Sox17 targets (C-E), Sox17 and Sox32 targets (F) and Sox32 targets (G-H); sample condition colour code and order of bars corresponds to the legend in panel B. Bar charts depict the mean fold change relative to uninjected controls, error bars ± one standard deviation, pink circles indicate individual datapoints. Statistical tests on biological triplicate samples were carried out using Student's t-test. * P<0.05.

321 during evolution led to differential Sox32 and Sox17 target specificity and induction.

322

323 **Sox17 is necessary for establishing correct brain, heart and pancreas laterality**

324 Given the distinct profile of Sox17 as a TF that is not merely redundant to Sox32,
325 what is the full biological scope of its function? Organ development requires not only
326 endoderm specification, but also subsequent tissue placement. For many species'
327 organ systems, bilateral asymmetry is vital for correct function, including in humans
328 (Sutherland and Ware 2009; Agarwal, et al. 2021). Heterotaxia is a syndrome of
329 abnormal abdominal and thoracic organ placement across the left-right axis of the

330 body, including the pancreas and heart (Aiello, et al. 2007). In the brain, similar defects
331 can alter patterns of gene expression and affect neural connectivity (Bianco and Wilson
332 2008).

333 Zebrafish Sox17 has previously been implicated in the establishment of LR
334 asymmetry. Knockdown of Sox17 using an antisense morpholino (MO) was previously
335 reported to result in abnormal pancreas placement, which could be rescued by co-
336 injection with *sox17* mRNA to which the morpholino did not bind (Aamar and Dawid
337 2010). However, an analysis of zebrafish *sox17* function in genetic mutants is lacking.
338 Furthermore, we aim to identify key domains of Sox17 required for correct LR
339 patterning.

340 To further explore the role of Sox17 in LR asymmetry we used an efficient
341 method of G0 CRISPR (Wu, et al. 2018) (Supplementary Figure S6) to disrupt the
342 *sox17* locus by injection of Cas9-sgRNA complexes at the one-cell stage. We then
343 analysed LR patterning using whole mount *in situ* hybridisation (WISH) of marker
344 genes. We assessed organ placement for the normally dextrally looped heart
345 (myocardial marker *myl7*, (Bakkers 2011) (Yelon, et al. 1999)), dextrally positioned
346 pancreas (*insulin* expression, (Argenton, et al. 1999)), and sinistrally stronger gene
347 expression in the habenular nuclei of the brain (*kctd12.1* expression, (Concha and
348 Wilson 2001) (Sutherland 1982) (Gamse, et al. 2003; Gamse, et al. 2005)) (Figure 6A).

349 We find that Sox17 CRISPants show abnormal brain asymmetry, heart looping
350 and pancreas placement (Figure 6B-D). This includes a significant increase in the
351 proportion of embryos exhibiting a middle and left-sided pancreas compared to the
352 control (Figure 6B. We co-injected *sox17* mRNA into CRISPants at the one-cell stage
353 to assess its ability to rescue the observed phenotypes. This resulted in a significant
354 increase in embryos with normal right-sided pancreas placement. This occurred
355 concurrently with a significant decrease in middle placement, while aberrant left-sided
356 placement remained unaffected (Figure 6B). This indicates that the middle placement
357 of the pancreas can be rescued by exogenous *sox17* mRNA, however left-sided
358 pancreas, *i.e.*, total reversal, cannot.

359 Neither brain asymmetry (Figure 6C) nor heart looping (Figure 6D) could be
360 rescued by co-injection of exogenous *sox17* mRNA into CRISPants. To test whether
361 exogenous Sox17 itself may be affecting LR patterning, we carried out OE studies
362 through the injection of *sox17* mRNA across a broad range of concentrations. This
363 indicated that Sox17 OE does not alter either brain asymmetry or heart looping

364 (Supplementary Figure S7). The lack of rescue of abnormal phenotypes is therefore
365 not due to the effect of Sox17 OE.

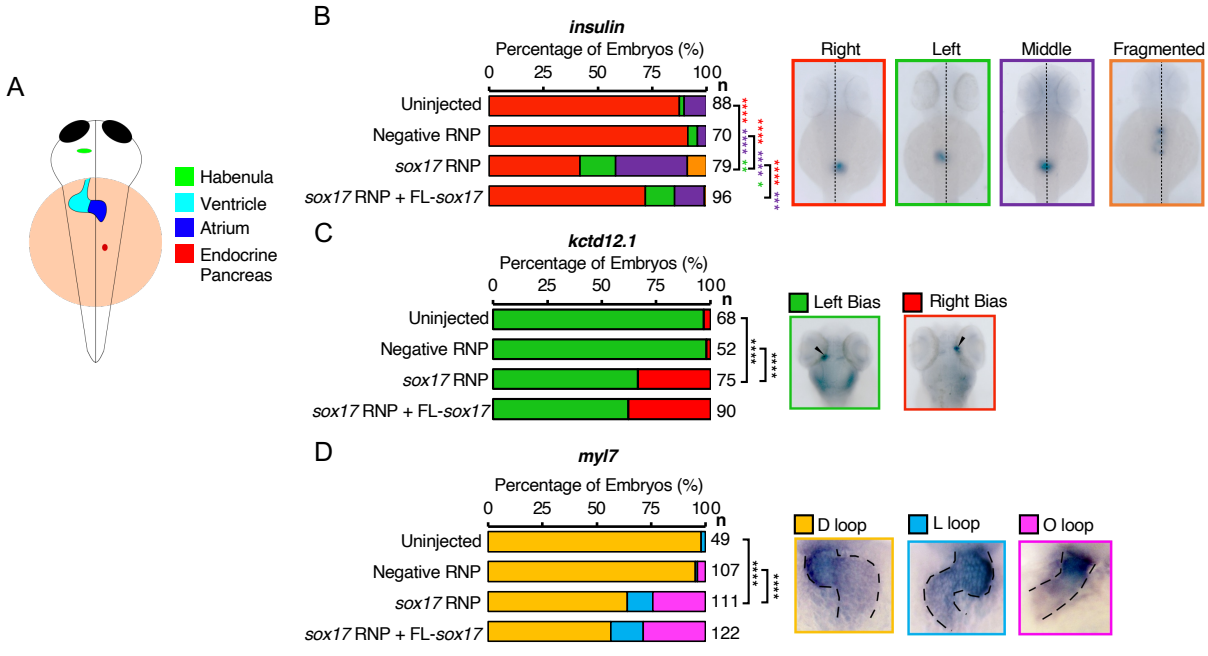

366

Figure 6: Sox17 CRISPants exhibit left-right asymmetry defects. A) Diagram depicting correct asymmetry of organs (4 days post-fertilisation - dpf). *Ktcd12.1* expression in the brain shows a left habenulae bias (green). The heart loops in a dextral (D-loop) fashion (blue). The endocrine pancreas is located to the right of the midline (red). **B-D)** WISH analysing the effect of Sox17 knockdown on endocrine pancreas placement relative to the midline (dotted line) at 48 hpf indicated by *insulin* (B); dorsal habenula *kctd12.1* asymmetric expression at 4 dpf – arrowheads indicate highest habenula expression (C); and heart looping at 48 hpf indicated by *myl7* – expression domain is outlined to highlight looping (D). Also shown are the phenotypic outcomes from rescue experiments from the co-injection of *sox17* exogenous mRNA along with CRISPR RNPs at the one-cell stage. Statistically significant differences in categorical scoring were inferred using Fisher's Exact test on independent biological triplicate datasets. * $P < 0.05$, ** $P < 0.01$, *** $P < 0.001$, **** $P < 0.0001$. For B) red asterisks indicate a significant difference in right-sided pancreas *vs.* all other phenotypic outcomes, purple asterisks indicate a significant difference between middle-placed pancreas *vs.* everything else and green asterisks indicate a significant difference between left-sided pancreas and everything else. For C-D) black asterisks indicate significant difference between normal laterality and all other phenotypes. n= the number of embryos analysed.
367

368 Going further, we considered whether the failure of *sox17* mRNA injection to
369 rescue heart looping was due to underlying defects in adjacent tissue patterning.
370 Sox32 mutants that lack anterior endoderm exhibit *cardia bifida* (Alexander, et al.
371 1999), a condition in which independent left and right heart fields develop due to a
372 failure of coalescing morphogenesis. We therefore analysed our Sox17 CRISPants for
373 expression of the anterior endoderm markers *foxa2* and *vgll4l.* Contrary to the reported
374 Sox17 MO phenotype (Aamar and Dawid 2010), we found that the anterior endoderm
375 is intact in Sox17 CRISPants (Supplementary Figure S8). Therefore, the lack of rescue
376 of heart looping does not appear to be a secondary effect due to endoderm defects.

377 The failure of exogenous *sox17* mRNA to rescue defective pancreas
378 positioning, brain asymmetry or heart looping led us to test whether KV function can
379 be rescued. A key early step in the establishment of LR asymmetry, which is indicative
380 of KV function, is unilateral *spaw* expression in the left LPM. Consistent with a defects
381 in organ placement, we found that exogenous *sox17* mRNA injection at the one-cell
382 stage failed to restore left-sided *spaw* expression in Sox17 CRISPants at 18 hpf
383 (Supplementary Figure S9). This suggests that KV function is not restored by
384 exogenous *sox17* mRNA. Since exogenous *sox17* mRNA is sufficient to restore right-
385 sided placement of a proportion of pancreases that are aberrantly placed at the midline
386 in Sox17 CRISPants, this suggests reduction of aberrant middle pancreas placement
387 is independent of KV.
388 In conclusion, we have shown that Sox17 CRISPants have abnormalities in
389 brain asymmetry, heart looping and pancreas placement. Only abnormal middle placed
390 pancreas can be rescued by co-injection of the *sox17* mRNA into CRISPants. The
391 placement of the pancreas is determined by looping of the posterior foregut as a result
392 of LPM migration, in which *sox17* is also expressed (Horne-Badovinac, et al. 2003;
393 Chung, et al. 2011). Therefore, Sox17 likely has a role in gut looping that exogenous
394 *sox17* mRNA is sufficient to rescue, which we speculate may be linked to a function in
395 the LPM.
396
397 **Conserved C-terminal peptides are required in Sox17 for correct pancreas**
398 **placement**
399 We have confirmed that Sox17 is required for organ asymmetry in zebrafish and
400 that we can rescue pancreas placement through co-injection of *sox17* mRNA into
401 CRISPants. We can therefore use this system to molecularly dissect which domains
402 of Sox17 are required for its role in this process. We created *Sox17* mutant constructs
403 with selected deletions based on high-level conservation among teleost and
404 mammalian Sox17 orthologues (Supplementary Figure S10). Four conserved regions
405 were identified and deleted: the Sox17 NTD, and three distinct regions within the CTD
406 of varying lengths (Figure 7A: 35 aa, 14 aa and 20 aa). The mRNA corresponding to
407 each mutant construct was injected into *sox17* CRISPants at the one-cell stage and
408 their capacity to rescue correct pancreas placement was assessed.

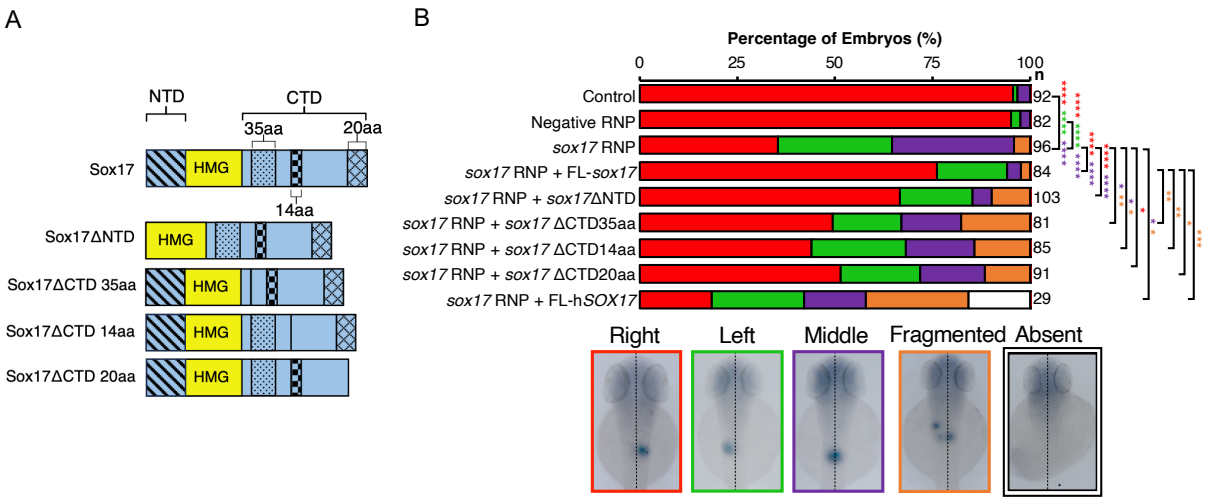

Figure 7: Sox17 CTD peptides are required for rescue of correct pancreas placement in Sox17 CRISPants. A) Diagram depicting protein models of Sox17 mutants. **B)** WISH at 48 hpf using *insulin* to assess the ability of Sox17 mutants in rescuing abnormal exocrine pancreas placement by co-injection of *sox17* exogenous mRNA alongside CRISPR RNPs at the one-cell stage. Statistically significant differences in categorical scoring were inferred using Fisher's Exact test on independent biological triplicate datasets. * = P<0.05, ** = P<0.01, *** = P<0.001, **** = P<0.0001. Red asterisks indicate a significant difference in right-sided pancreas *vs.* all other phenotypes, purple asterisks indicate a significant difference between middle-placed pancreas *vs.* all other phenotypes, green asterisks indicate a significant difference between left-sided pancreas *vs.* all other phenotypes and yellow asterisks indicate a significant difference between fragmented *insulin*+ domains *vs.* all other phenotypes. FL refers to full length. n= the number of embryos analysed.

We find that Sox17ΔNTD can rescue pancreas placement in *sox17* CRISPants to a similar degree as full length (FL)-Sox17. Both constructs result in a significant increase in CRISPants exhibiting normal right-sided pancreas placement and a significant decrease in embryos showing middle placement, with left-sided placement unaffected compared to *sox17* CRISPants alone (Figure 7B). This indicates the N-terminal domain of Sox17 is largely dispensable for its function in pancreas placement.

Sox17ΔCTD35aa and Sox17ΔCTD14aa mRNA injections lead to a significant decrease in *sox17* CRISPant embryos with a middle-placed pancreas. However, this does not coincide with an increase in normal right-sided placement as seen with FL-Sox17 and Sox17ΔNTD. Instead, there is a significant increase in embryos exhibiting multiple fragmented *insulin*+ domains (Figure 7B). Sox17ΔCTD20aa mRNA injection leads to a significant increase in CRISPants with normal right-sided placement compared to embryos injected with *sox17* RNP alone, suggesting this mutant construct retains some degree of relevant function. However, we also note that we reduction in aberrant pancreas placement is also accompanied by a moderate increase in pancreas fragmentation (Figure 7B). Overall, all three CTD mutants may have some reduced

426 capability to restore migration of the pancreas to the right, though not to the degree of
427 FL-Sox17 and Sox17ΔNTD. However, the CTD mutants also disrupt pancreas
428 formation, either by driving ectopic specification of pancreas identity, or migration
429 defects leading to the fragmented phenotype observed.

430 *Sox17*$^{-/-}$ mutant mice exhibit an open body wall and failure to turn from a
431 concave to a convex "foetal" position (Kanai-Azuma, et al. 2002; Viotti, et al. 2012) –
432 characteristics of mutants with LR patterning defects (Hamada, et al. 2002). Given the
433 requirement for Sox17 in LR patterning in mammals and zebrafish, we sought to
434 determine whether mammalian SOX17 has the capacity to induce correct pancreas
435 placement through injection of h*SOX17* mRNA into *sox17* CRISPants. We found that
436 hSOX17 is unable to rescue pancreas placement. Instead, it leads to a further
437 decrease in right-sided pancreas placement in CRISPants, or even the total absence
438 of the pancreas (Figure 7B). The aberrant LR phenotype in mouse has been suggested
439 to be largely a secondary effect due to depletion of gut endoderm (Viotti, et al. 2012),
440 while zebrafish Sox17 CRISPants do not exhibit loss of endoderm (Supplementary
441 Figure S7). Taken together, this indicates that while Sox17 is required for LR
442 asymmetry in mammals and zebrafish, mechanistic variability exists.

443 Overall, we conclude the Sox17 CTD is required for correct pancreas
444 placement, while the NTD is dispensable. Additionally, our results indicate that
445 peptides in the CTD can influence formation of an intact endocrine pancreas, although
446 whether this reflects aberrant morphogenesis or specification is unclear.

447 Taken together, our results reveal the molecular basis for functional divergence
448 between Sox17 and Sox32, highlighting key functional peptides controlling both
449 endoderm and DFC specification, and the establishment of pancreas placement during
450 gut morphogenesis.

451

452 **Discussion**

453 A classical view of the fate of duplicated genes that remain functional during
454 evolution is that they either undergo sub- or neofunctionalization (Tasnim, et al. 2024).
455 How does the case of Sox17 and Sox32 reflect this? The expression domains of *sox32*
456 and *sox17* substantially overlap in the early embryo with Sox32 activating *sox17*
457 expression, and are similar to *Sox17* expression patterns in other species. We
458 therefore consider sub- or neofunctionalization in the context of protein function rather
459 than expression domains.

460

461 **Divergence of the Sox32 HMG domain is critical to allow engagement with the**
462 **teleost endoderm GRN**

463 Consistent with previous reports (Kikuchi, et al. 2001; Stafford, et al. 2006) our
464 analyses indicate that ectopic Sox32 expression induces endodermal cell identity at
465 the expense of other cell types, indicating its ability to change cell fate (Figure 3G).
466 Remarkably, it also induces a significant number of DFC marker genes suggesting that
467 while Sox32 is necessary for DFC identity it is also substantially sufficient to direct the
468 DFC gene expression programme (Figure 3G).

469 Our molecular analyses reveal that the ability of Sox32 to orchestrate the
470 endoderm GRN is dependent on differences between the Sox32 and Sox17 HMG
471 domains. Given the greater similarity between Sox17 and hSOX17 HMG domains, we
472 suggest Sox32 diverged after the duplication event where *sox32* and *sox17* emerged.
473 This suggests a scenario wherein subfunctionalisation has occurred with Sox32
474 adopting the key role in endoderm formation, while Sox17 retains other roles such as
475 regulating genes involved in vasculogenesis, as SOX17 does in mammals (Figures
476 S2, S4). However, the divergence of the Sox32 HMG domain and the inability of
477 hSOX17 to induce endoderm marker expression in zebrafish raises questions about
478 the mechanistic similarities by which these TFs orchestrate endoderm gene expression
479 in their native species. It is possible that the different HMG domains bind different *cis*-
480 regulatory modules (CRMs) and hence activate different downstream target genes in
481 our experiments, either due to different DNA binding preferences or altered
482 physiochemical interactions with co-factors. However, all Sox TFs are considered to
483 individually bind similar sequence motifs (Kondoh and Kamachi 2010). Furthermore,
484 contact sites between mouse SOX17 HMG domain and a *cis*-regulatory enhancer
485 upstream of the *Lama1* transcriptional start site have been mapped (Palasingam, et
486 al. 2009) and are highly conserved in Sox32 and Sox17 (Figure 2D). This may indicate
487 that Sox32, Sox17 and hSOX17 HMG domains are individually capable of engaging
488 similar DNA sequences. A more likely scenario is that the differences between HMG
489 domains alters the spectrum or configuration of co-factor interactions, impacting co-
490 operative engagement of TF complexes with CRMs. However, it does not necessarily
491 follow that hSOX17 and Sox32 have substantially different co-factors during endoderm
492 formation if orthologous co-factors have undergone parallel evolution. In this scenario
493 hSOX17 and Sox32 would only be able to interact with co-factors from their native

494 species, which would preclude hSOX17 from inducing endoderm marker expression
495 in zebrafish. It would also explain why the Sox17 HMG domain cannot substantially
496 engage the endoderm GRN, if key co-factors have evolved to engage Sox32.
497 While very few Sox32 interacting TFs have been identified, an interesting
498 candidate that may explain the differences in HMG domain functions is the TF Pou5f3.
499 Pou5f3 is required for Sox32-mediated induction of endoderm fate (Lunde, et al. 2004;
500 Reim, et al. 2004; Zhao, et al. 2013). However, in mammals the SOX17 HMG domain
501 interacts with the POU domain of POU5F1 to cooperatively bind CRMs and orchestrate
502 target gene induction (Stefanovic, et al. 2009; Ng, et al. 2012). While not true
503 orthologues, human *POU5F1* is the closest homologue of zebrafish *pou5f3*.
504 Duplication of an ancestral *Pou5* gene occurred in the last common ancestor of extant
505 cartilaginous fishes and bony fishes leading to two genes. Subsequent gene loss has
506 led to maintenance of only *pou5f3* in teleosts and *POU5F1* in eutherians including
507 humans (Frankenberg and Renfree 2013). POU5F1 (also known as OCT3 or OCT4)
508 is known to interact with the HMG domains of many SOX factors (Ng, et al. 2012).
509 However, distinctions between HMG domains leads to alterations in POU5F1
510 engagement, and consequently different SOX-POU5F1 target sequence selection (Ng,
511 et al. 2012). Thus, altered configuration of Sox32-Pou5f3 interactions compared to
512 SOX17-POU5F1 would likely prevent engagement with the same CRMs. Similarly, the
513 requirement for correct partner cooperation in target transcription has been established
514 in human SOX TF function. For example, SOX2 can interact with both OCT3 and
515 OCT1, but only the SOX2-OCT3 complex can promote transcriptional activation of the
516 FGF4 enhancer (Yuan, et al. 1995). It is therefore likely that Sox32 complexes have
517 different sequence specificities to Sox17- or hSOX17-containing complexes, either
518 through altered interaction with the same/homologous co-factors or altered co-factor
519 selection. This would lead to different target site selection and distinct functional
520 outcomes for SOX factors that are otherwise capable of binding the same individual
521 consensus sequence. Future analyses should therefore focus on the interacting
522 partners and DNA binding preferences of resulting Sox TF complexes, and whether
523 hSOX17 and Sox32 have demonstrably similar or distinct target CRMs in their native
524 species.
525
526
527

528 **Functional partition and divergence through alteration of C-terminal helices**

529 A key distinction between these endoderm-relevant SoxF factors is a putative
530 CTD helix, which is notably longer in Sox32 than Sox17 (Figure 2A-C). The 25-aa high
531 confidence prediction in Sox32 (Figure 2A) encompasses a short peptide (EFDQYL)
532 which deviates from hSOX17 by only a single amino acid of similar properties
533 (EFEQYL). Importantly, this EF(D/E)QYL motif was first identified in *Xenopus* where
534 Sox17α shows 100% sequence identity to hSOX17 and Sox17β to Sox32, with both
535 peptides critical to Sox17α/β interaction with Wnt pathway effector β-catenin (Sinner,
536 et al. 2004). Additionally, *Xenopus* Sox17α/β and hSOX17 co-occupy enhancers with
537 β-catenin resulting in activation of endoderm-specific genes and repression of
538 mesoectodermal genes (Mukherjee, et al. 2020; Mukherjee, et al. 2022). However,
539 zebrafish Sox17 exhibits alterations in this peptide including replacement of the central
540 polar uncharged glutamine (Q) residue with a positively charged histidine (H) residue,
541 and also substitution of the polar amino acid tyrosine (Y) for non-polar cysteine (C)
542 (Figure 2E). It is therefore likely that Sox32 has retained the ancestral function of
543 recruiting β-catenin to activate endoderm-specific genes, while divergence of this
544 peptide in Sox17 has led to neofunctionalisation. This is supported by our observation
545 that both Sox32 and Sox17 require their own individual peptide sequences (EFDQYLN
546 and EFEHCLS respectfully as tested) for induction of their distinct target genes. Thus,
547 the function of Sox32 in directing the endoderm GRN relies on divergence of its HMG
548 domain and retention of the C-terminal β-catenin interacting peptide, while alterations
549 to this C-terminal peptide in Sox17 likely led to altered target gene selection and
550 consequent functional diversification.

551 The 25-aa CTD helical domain in Sox32 contains 18 aa upstream of the β-
552 catenin interacting peptide. Our analyses (via deletion of a 23 aa peptide
553 encompassing the 18-aa helix and five upstream amino acids) indicates that this
554 broader helical domain is also essential for Sox32-mediated induction of endoderm
555 and DFC target genes (Figure 4). Additionally, though Sox17 requires its divergent
556 EFEHCLS peptide for induction of its target genes, substitution for the Sox32 25-aa
557 CTD helical domain nevertheless leads to potent induction of Sox17 (though not
558 Sox32) target genes (Figure 5D-E). We therefore hypothesise the Sox32 CTD helix is
559 a potent transactivation domain. Interestingly, C-terminal helices in FoxA factors have
560 been shown to be critical for gene activation, facilitating binding to histone octamers

561 leading to nucleosome eviction and increased chromatin accessibility (Pani, et al.
562 1992; Iwafuchi, et al. 2020). It would be interesting to determine whether the 25 aa
563 CTD helix in Sox32 similarly confers pioneer TF activity.
564
565 **Sox17 potentially has multiple roles in establishing organ asymmetry**
566 Our analyses of G0 CRISPants suggests Sox17 is necessary for correct
567 unilateral Nodal (*spaw*) expression, brain asymmetry, heart looping and pancreas
568 placement (Figure 6). Furthermore, we have shown that co-injection with exogenous
569 *sox17* mRNA is sufficient to rescue abnormal pancreas placement phenotypes in
570 Sox17 CRISPants, consistent with previous experiments with antisense morpholinos
571 (Aamar and Dawid 2010). However, exogenous *sox17* mRNA is not sufficient to rescue
572 abnormal Nodal expression, heart looping or brain asymmetry. This tantalisingly
573 suggests Sox17 may have distinct roles in different cell types to establish organ
574 asymmetry, as we discuss below.
575 The process of zebrafish heart morphogenesis and looping has been
576 extensively studied and reviewed (Bakkers 2011). While we have shown that an intact
577 *sox17* locus is necessary for correct zebrafish heart looping, the lack of phenotypic
578 rescue by exogenous *sox17* mRNA cannot be attributed to injection of exogenous
579 *sox17* mRNA (Supplementary Figure S7), or a secondary consequence of an
580 endodermal phenotype (Supplementary Figure S8). Our RNA-seq analyses show
581 Sox17-induced genes are enriched for heart-related anatomical terms, including
582 endocardium and ventricular myocardium (Supplementary Figure S2). Additionally, we
583 have observed *sox17:EGFP* reporter expression in the heart including in the
584 endocardium, based on co-expression with *kdrl:mCherry* (Supplementary Figure S4A,
585 Video S1). These cells arise from precursors in the LPM, which is *sox17*+ (Zhong, et
586 al. 2001; Chung, et al. 2011). *Sox17* is expressed in mouse endocardium, where it is
587 required for proper heart morphogenesis (Saba, et al. 2019). Considering we find
588 *sox17:EGFP*+ cells within the zebrafish heart (Supplementary Figure S4), a conserved
589 role within the endocardium controlling heart morphogenesis is plausible.
590 Sox17 is also expressed within KV (Schneider, et al. 2008; Chung, et al. 2011),
591 and morpholino knockdown of Sox17 leads to abnormality in KV morphogenesis and
592 function via defective ciliogenesis (Aamar and Dawid 2010). The perturbation of cilia
593 function results in aberrant *spaw* expression within the LPM (Kramer-Zucker, et al.
594 2005). We show that Sox17 CRISPants exhibit aberrant *spaw* expression in the LPM,

595 and this cannot be restored to normal left-sided *spaw* expression through co-injection
596 of exogenous *sox17* mRNA (Supplementary Figure S9). This suggests we are not able
597 to rescue KV function with exogenous *sox17* mRNA, leading to an inability to rescue
598 correct brain asymmetry and heart looping. An explanation may be off-target disruption
599 of another gene acting in KV function. However, this seems unlikely given morpholino
600 knockdown of Sox17 also leads to KV defects (Aamar and Dawid 2010). Alternatively,
601 since KV typically consists of ~50 cells (Gokey, et al. 2016) – a tiny proportion of the
602 embryo – it is possible that the failure to rescue left-sided *spaw* expression is due to a
603 lack of inheritance of exogenous *sox17* mRNA by sufficient KV cells, as *sox17* OE itself
604 does not lead to LR defects (Supplementary Figure S7).
605 However, the failure to rescue KV function (and thus brain asymmetry and heart
606 looping) makes the rescue of pancreas placement even more tantalising. As well as
607 KV function, visceral organ laterality and therefore pancreas placement is also
608 determined by LPM migration, which pushes the developing pancreas to the right of
609 the midline due to left-sided Nodal signalling (Horne-Badovinac, et al. 2003).
610 Alterations in Nodal signalling within the LPM randomises the pattern of LPM migration,
611 resulting in aberrant pancreas placement (Horne-Badovinac, et al. 2003). Remarkably,
612 however, exogenous *sox17* mRNA can restore gut looping in Sox17 CRISPants as
613 indicated by a significant reduction in midline-placed pancreas, even though it cannot
614 rescue KV function (Figure 6B). Since *sox17* is expressed in LPM (Chung, et al. 2011),
615 this suggests that LPM migration is compromised in Sox17 CRISPants, but can be
616 restored through exogenous *sox17* mRNA injection. It is tempting to speculate that
617 the fragmented pancreas phenotype we observe on mutant *sox17* mRNA injection also
618 reflects effects on LPM migration (though ectopic pancreas specification is also a
619 possibility). Overall, our data confirms Sox17 controls LR asymmetry through roles in
620 KV, and suggests a new role for Sox17 in gut looping and possibly also in heart looping
621 through expression in the endocardium. Our analyses show that multiple peptides
622 conserved among Sox17 orthologues are required for rescue of the pancreas
623 placement defect in Sox17 CRISPants. Strikingly, amongst these is the Sox17CTDΔ14
624 aa deletion which encompasses the EFEHCLS sequence noted to have diverged from
625 the ancestral β-catenin interacting peptide. It is therefore possible that this divergence
626 of Sox17 is key to its role in controlling gut looping in zebrafish.
627

628 Overall our results indicate that evolutionary alterations in the HMG domain of
629 Sox32 combined with the presence of a CTD helical domain including retention of a β-
630 catenin interacting peptide are key to its orchestration of the endoderm and DFC
631 GRNs. While hSOX17 clearly cannot engage the zebrafish endoderm GRN in the
632 context of these experiments, it would be interesting to explore whether Sox32 and
633 hSOX17 have similar target genes and co-factors within their native species. In
634 contrast to Sox32, alterations in the CTD of Sox17 have driven functional divergence.
635 This alters target gene specificity in the early embryo and may be related to a new
636 function for Sox17 in controlling gut looping to establish visceral organ asymmetry,
637 which warrants further in-depth investigation.
638
639
640 **Materials and Methods**
641 Animals
642 AB, *Tg(sox17:EGFP)*^{ha01Tg} and *Tg(kdrl:mCherry*^{S896}*,gata1a:dsRed*^{sd2tg}*)* fish
643 were reared as described (Westerfield 2000; Traver, et al. 2003; Chi, et al. 2008;
644 Mizoguchi, et al. 2008). All zebrafish studies were conducted in compliance with the
645 United Kingdom Animals (Scientific Procedures) Act 1986, licensed by the UK Home
646 Office and implemented by The University of Warwick.
647
648 Confocal Microscopy
649 48 hpf zebrafish embryos were anesthetized with 0.168%(w/v) of Ethyl 3-
650 aminobenzoate methanesulfonate, prior to mounting in 1% lateral view agarose
651 moulds. Moulds were generated from a 3D stamp as designed by (Kleinhans and
652 Lecaudey 2019). To ensure high-quality imaging, embryos were treated before 24 hpf
653 with 0.003% (w/v) 1-Phenyl-2-thiourea (PTU) to prevent pigmentation (Karlsson, et al.
654 2001). Imaging was carried out on a Zeiss LSM 980 with Airyscan 2.
655
656 Cloning for *in vitro* production of mRNAs
657 pCS2+*hSOX17* was cloned from PB-TRE3G-SOX17 (Miller, et al. 2018) using
658 XhoI and XbaI restriction sites. PB-TRE3G-SOX17 was a gift from David Vereide
659 (Addgene plasmid # 104541; http://n2t.net/addgene:104541; RRID:Addgene_104541)
660 *Sox17* and *sox32* deletion and domain switch constructs (Supplementary Table
661 S11) were generated using pCS2+*sox17* and pCS2+*myc-sox32* by PCR amplification
662 using Q5 polymerase (NEB) with described primers (Supplementary Table S12)
663 followed by re-circularisation or insertion using T4 ligase (Invitrogen). All constructs
664 were generated using blunt-end cloning, except for Sox17Δ7aa + Sox32 25aa and
665 Sox32ΔHMG + Sox17 HMG where NEBuilder HiFi DNA Assembly (NEB), with
666 Sox17Δ7aa + Sox32 25aa as a gBlock (Integrated DNA Technologies) was used.
667
668 mRNA *in vitro* transcription
669 Capped mRNA was synthesised from pCS2+ plasmids containing genes of
670 interest. Linearisation with NotI was conducted followed by transcription using SP6
671 RNA polymerase as previously described (Talbot, et al. 2022).

672
673 Ribonuclear protein (RNP) complex production
674 To knockdown *sox17* ribonucleoprotein (RNP) complexes were generated using
675 a pool of three guide RNAs and Cas9 protein (Integrated DNA Technologies) as
676 described (Essner 2016). Guide RNAs that do not target the zebrafish genome were
677 used to generate a negative control RNP. Guide RNAs were generated from specific
678 crRNAs (Supplementary Table S13) and standard tracrRNA (Integrated DNA
679 Technologies) as described (Essner 2016). crRNAs against *sox17* were predesigned
680 by Integrated DNA Technologies and selected based on predicted on-target and off-
681 target scores from both Integrated DNA Technologies and CHOPCHOP (Labun, et al.
682 2019).
683
684 Microinjection
685 Equimolar amounts of mRNA (calculated based on relative mRNA length) were
686 injected at the one-cell stage. For interspecies RNA-seq each embryo was injected
687 with the following amount: *sox32* – 150pg, h*SOX17* – 141pg, *sox17* – 175pg. For HMG
688 Switch RNA-seq each embryo was injected with the following amount: *sox32* – 150pg,
689 *sox32*ΔHMG – 121.5pg, and *sox32*ΔHMG+*sox17*HMG – 148.5pg. For *sox32* mutant
690 qPCR, each embryo was injected with the following amount: *sox32* – 150pg, -
691 *sox32*ΔNTD – 127.5pg, *sox32*ΔHMG – 121.5pg, *sox32*ΔCTD23aa – 142.5pg,
692 *sox32*ΔCTD7aa – 147pg. For CTD switch qPCR, each embryo was injected with the
693 following amount: *sox17* – 150pg, *sox17*Δ7aa – 147pg, *sox32* – 128ng,
694 *sox32*Δ7aa+*sox17*-7aa – 128pg, *sox17*Δ7aa+*sox32*-7aa – 150pg, *sox17*Δ7aa+*sox32*-
695 25aa – 155pg. For Sox17 functional dissection, each embryo was injected with the
696 following amount of mRNA: *sox17* – 150pg, *sox17*ΔNTD – 134pg, *sox17*ΔCTD35aa –
697 139pg, *sox17*ΔCTD14aa – 145pg, *sox17*ΔCTD20aa – 143pg, h*SOX17* – 108pg. For
698 overexpression experiments mRNA was injected in a volume of 1nL. To produce
699 CRISPant embryos RNPs were injected in a volume of 3nL. For experiments involving
700 combined CRISPR RNP and mRNA injection RNPs and mRNAs were injected in a
701 combined volume of 4nL.
702
703 Whole mount *in situ* hybridisation (WISH)
704 WISH of zebrafish embryos was carried out as described (Thisse and Thisse
705 2008). Anti-sense RNA probes for *myl7* (Yelon, et al. 1999), *insulin* (Milewski, et al.
706 1998), *vgll4l* (Nelson, et al. 2014) and *foxa2* (Odenthal and Nüsslein-Volhard 1998)
707 were synthesised as described. *Ktcd12.1* RNA probe was generated from a PCR
708 product using primers: F - CTGCCGGACTATTTTCCAGAG, R-
709 TAATACGACTCACTATAGGGAGCTGCACGCGACCATCT and transcribed using T7
710 polymerase (Promega). Categorical scoring on randomised samples was completed
711 blinded.
712
713 Total RNA Extraction
714 Embryos were lysed at 6 hpf via addition of 600ul buffer RLT and DTT (2% v/v)
715 to at least fifty embryos per condition, with initial disruption using a plastic pestle.
716 Further disruption was carried out using QIAshredder columns (QIAGEN) and RNA
717 was extracted using the RNeasy Mini Kit (QIAGEN) with on-column DNase treatment
718 (QIAGEN) as per manufacturer's protocol.
719
720 qPCR

721 cDNA was generated from 400ng of total RNA using Random Hexamers
722 (Promega) and Ultrascript Reverse Transcriptase (PCR Bio) as per manufacturer's
723 protocol. qPCR was carried out using relevant primers (Supplementary Table S14) and
724 Power SYBR Green Master Mix (Thermofisher) on the Stratagene Mx3005P (Agilent
725 Technologies). Raw Ct values were extracted using MxPro software and analysed
726 using the ΔΔCt method (Livak and Schmittgen 2001), with normalisation to *18S* rRNA
727 (McCurley and Callard 2008). Statistical differences were inferred using Students t-test
728 with significance set at $P < 0.05$.
729
730 RNA-sequencing Library Preparation and Analysis
731 Total RNA was sent to the Cologne Center for Genomics (CCG) for library
732 preparation (Illumina TruSeq Stranded mRNA) and sequencing on the Illumina
733 NovaSeq 6000 platform with a read length of 101 bp.
734 Quality control of raw data was performed using FastQC. Reads were mapped
735 to danRer11 zebrafish genome and counts per gene (Ensembl version 97) generated
736 using STAR with default settings (Dobin, et al. 2013). Differential expression was
737 identified through adjusted P-value < 0.05 using DESeq2 (1.36.0) (Love, et al. 2014)
738 in R (4.2.0). To identify whether different TFs illicit similar or different effects on the
739 transcriptome, upregulated and downregulated DEGs were separately overlapped to
740 identify whether TFs induce or repress similar genes. Statistical testing to identify
741 whether the overlap in genes was significantly more/less than expected by chance was
742 conducted using Fisher's exact test (phyper in R). This analysis used a gene universe
743 size defined as all genes detected in RNA-seq where samples in all conditions showed
744 counts > 0. Heatmaps were generated on median normalised counts per condition
745 using pheatmap (1.0.12) with 'scale = row' option to display deviation in expression
746 from the average expression of each gene. Gene Ontology (GO) and anatomy term
747 enrichment analysis was carried out on fishEnrichR (Chen, et al. 2013; Kuleshov, et al.
748 2016) using autoRIF Z-score, with significantly enriched terms defined by an adjusted
749 P-value < 0.05.
750 To infer how TFs influence cell fate, Gene Set Enrichment Analysis (GSEA) was
751 carried out using published scRNA-sequencing data (Wagner, et al. 2018) as cell
752 identity markers using GSEA (4.3.2) (Mootha, et al. 2003; Subramanian, et al. 2005).
753
754 Conservation Analysis
755 Protein sequences were obtained from UniProt (The UniProt 2023)
756 (Supplementary Table S15) and alignments were conducted aligned using Clustal
757 Omega in JalView (Sievers, et al. 2011; Sievers and Higgins 2018). Jalview uses
758 multiple sequence alignments according to Analysis of Multiply Aligned Sequences
759 (AMAS) (Livingstone and Barton 1993) to calculate conservation levels. Conserved
760 sequences were compared to 3D structures obtained from AlphaFold; Sox32
761 (Q90Z46), Sox17 (Q5PQZ5), hSOX17 (Q9H6I2) (Jumper, et al. 2021; Varadi, et al.
762 2022).
763
764 **Authors' contributions**
765 Conceived and designed the experiments: ACN, SJ, KAP. Performed the experiments:
766 SJ, RE. Analysed the data: SJ. Writing – original draft preparation: SJ. Writing – review
767 and editing: ACN, KAP.
768
769
770

Funding

This research was funded in whole or in part by the BBSRC Midlands Integrative Biosciences Training Partnership (BB/M01116X/1). This research was also funded, in part, by the Wellcome Trust through a Wellcome Seed Award in Science to ACN (210177/Z/18/Z); and by funding from the German Research Foundation (Deutsche Forschungsgemeinschaft) through SFB 680 project A12 to KAP. SJ has a PhD studentship funded by the BBSRC Midlands Integrative Biosciences Training Partnership (BB/M01116X/1). RE was funded by the MRC Doctoral Training Partnership in Interdisciplinary Biomedical Research (MR/N014294/1).

Acknowledgments

We thank Rui Monteiro for kindly gifting us the *Tg(kdrl:mCherry,gata1a:dsRed)* fish used in this study. We thank Fiona Wardle and Karuna Sampath for reagents. We thank Karuna Sampath, Emily Noël and Andre Pires da Silva for valuable discussions, and Karuna Sampath and Andre Pires da Silva for generous access to equipment. We thank Eirini Vlachaki for technical support early in the project. We also thank the Warwick zebrafish facility for zebrafish care and, Ian Hands-Portman from the Warwick School of Life Sciences for imaging advice and support.

Data Accessibility

All RNA-seq data have been submitted to NCBI Gene Expression Omnibus under accession number GSE274063.

References

Aamar E, Dawid IB. 2010. Sox17 and chordin are required for formation of Kupffer's vesicle and left-right asymmetry determination in zebrafish. Developmental dynamics : an official publication of the American Association of Anatomists 239:2980-2988.

Agarwal R, Varghese R, Jesudian V, Moses J. 2021. The heterotaxy syndrome: associated congenital heart defects and management. Indian Journal of Thoracic and Cardiovascular Surgery 37:67-81.

Aiello VD, Anderson RH, Béland MJ, Colan SD, Duca DD, Elliott MJ, Franklin RCG, Jacobs JP, Krogmann ON, Kurosawa H, et al. 2007. The nomenclature, definition and classification of cardiac structures in the setting of heterotaxy. Cardiology in the Young 17:1-28.

Alexander J, Rothenberg M, Henry GL, Stainier DYR. 1999. casanova Plays an early and essential role in endoderm formation in zebrafish. Developmental Biology.

Angelozzi M, Lefebvre V. 2019. SOXopathies: Growing Family of Developmental Disorders Due to SOX Mutations. Trends Genet 35:658-671.

Aoki TO, David NB, Minchiotti G, Saint-Etienne L, Dickmeis T, Persico GM, Strähle U, Mourrain P, Rosa FdrM. 2002. Molecular integration of casanova in the Nodal signalling pathway controlling endoderm formation. Development 129:275-286.

Argenton F, Zecchin E, Bortolussi M. 1999. Early appearance of pancreatic hormone-expressing cells in the zebrafish embryo. Mechanisms of Development 87:217-221.

Bakkers J. 2011. Zebrafish as a model to study cardiac development and human cardiac disease. Cardiovascular Research 91:279-288.

Bianco IH, Wilson SW. 2008. The habenular nuclei: a conserved asymmetric relay station in the vertebrate brain. Philosophical Transactions of the Royal Society B: Biological Sciences 364:1005-1020.

Bowles J, Schepers G, Koopman P. 2000. Phylogeny of the SOX Family of Developmental Transcription Factors Based on Sequence and Structural Indicators. Developmental Biology 227:239-255.
Chen EY, Tan CM, Kou Y, Duan Q, Wang Z, Meirelles GV, Clark NR, Ma'ayan A. 2013. Enrichr: interactive and collaborative HTML5 gene list enrichment analysis tool. BMC Bioinformatics 14:128.
Chi NC, Shaw RM, De Val S, Kang G, Jan LY, Black BL, Stainier DYR. 2008. Foxn4 directly regulates tbx2b expression and atrioventricular canal formation. Genes & development 22:734-739.
Chung MIS, Ma ACH, Fung T-K, Leung AYH. 2011. Characterization of Sry-related HMG box group F genes in zebrafish hematopoiesis. Experimental Hematology 39:986-998.e985.
Concha ML, Wilson SW. 2001. Asymmetry in the epithalamus of vertebrates. Journal of Anatomy 199:63-84.
Cooper MS, D'Amico LA. 1996. A Cluster of Noninvoluting Endocytic Cells at the Margin of the Zebrafish Blastoderm Marks the Site of Embryonic Shield Formation. Developmental Biology 180:184-198.
Dickmeis T, Mourrain P, Saint-Etienne L, Fischer N, Aanstad P, Clark M, Strähle U, Rosa F. 2001. A crucial component of the endoderm formation pathway, CASANOVA, is encoded by a novel sox-related gene. Genes & development 15:1487-1492.
Dobin A, Davis CA, Schlesinger F, Drenkow J, Zaleski C, Jha S, Batut P, Chaisson M, Gingeras TR. 2013. STAR: ultrafast universal RNA-seq aligner. Bioinformatics (Oxford, England) 29:15-21.
Essner JJ. 2016. Zebrafish embryo microinjection: Ribonucleoprotein delivery using the Alt-RTM CRISPR-Cas9 System. In.
Essner JJ, Amack JD, Nyholm MK, Harris EB, Yost HJ. 2005. Kupffer's vesicle is a ciliated organ of asymmetry in the zebrafish embryo that initiates left-right development of the brain, heart and gut. Development 132:1247 LP-1260.
Figiel DM, Elsayed R, Nelson AC. 2021. Investigating the molecular guts of endoderm formation using zebrafish. Brief Funct Genomics.
Frankenberg S, Renfree MB. 2013. On the origin of POU5F1. BMC Biol 11:56.
Gamse JT, Kuan Y-S, Macurak M, Brösamle C, Thisse B, Thisse C, Halpern ME. 2005. Directional asymmetry of the zebrafish epithalamus guides dorsoventral innervation of the midbrain target. Development 132:4869-4881.
Gamse JT, Thisse C, Thisse B, Halpern ME. 2003. The parapineal mediates left-right asymmetry in the zebrafish diencephalon. Development 130:1059-1068.
Gokey JJ, Ji Y, Tay HG, Litts B, Amack JD. 2016. Kupffer's vesicle size threshold for robust left-right patterning of the zebrafish embryo. Dev Dyn 245:22-33.
Gubbay J, Collignon J, Koopman P, Capel B, Economou A, Münsterberg A, Vivian N, Goodfellow P, Lovell-Badge R. 1990. A gene mapping to the sex-determining region of the mouse Y chromosome is a member of a novel family of embryonically expressed genes. Nature 346:245-250.
Hamada H, Meno C, Watanabe D, Saijoh Y. 2002. Establishment of vertebrate left–right asymmetry. Nature Reviews Genetics 3:103-113.
Horne-Badovinac S, Rebagliati M, Stainier DYR. 2003. A Cellular Framework for Gut-Looping Morphogenesis in Zebrafish. Science 302:662-665.
Iwafuchi M, Cuesta I, Donahue G, Takenaka N, Osipovich AB, Magnuson MA, Roder H, Seeholzer SH, Santisteban P, Zaret KS. 2020. Gene network transitions in embryos depend upon interactions between a pioneer transcription factor and core histones. Nature Genetics 52:418-427.

Jumper J, Evans R, Pritzel A, Green T, Figurnov M, Ronneberger O, Tunyasuvunakool K, Bates R, Žídek A, Potapenko A, et al. 2021. Highly accurate protein structure prediction with AlphaFold. Nature 596:583-589.
Kanai-Azuma M, Kanai Y, Gad JM, Tajima Y, Taya C, Kurohmaru M, Sanai Y, Yonekawa H, Yazaki K, Tam PPL, et al. 2002. Depletion of definitive gut endoderm in Sox17-null mutant mice. Development.
Karlsson J, von Hofsten J, Olsson P-E. 2001. Generating Transparent Zebrafish: A Refined Method to Improve Detection of Gene Expression During Embryonic Development. Marine Biotechnology 3:522-527.
Kikuchi Y, Agathon A, Alexander J, Thisse C, Waldron S, Yelon D, Thisse B, Stainier DYR. 2001. casanova encodes a novel Sox-related protein necessary and sufficient for early endoderm formation in zebrafish. Genes and Development.
Kikuchi Y, Trinh LA, Reiter JF, Alexander J, Yelon D, Stainier DYR. 2000. The zebrafish bonnie and clyde gene encodes a Mix family homeodomain protein that regulates the generation of endodermal precursors. Genes and Development.
Kleinhans DS, Lecaudey V. 2019. Standardized mounting method of (zebrafish) embryos using a 3D-printed stamp for high-content, semi-automated confocal imaging. BMC Biotechnology 19:68.
Kondoh H, Kamachi Y. 2010. SOX-partner code for cell specification: Regulatory target selection and underlying molecular mechanisms. Int J Biochem Cell Biol 42:391-399.
Kramer-Zucker AG, Olale F, Haycraft CJ, Yoder BK, Schier AF, Drummond IA. 2005. Cilia-driven fluid flow in the zebrafish pronephros, brain and Kupffer's vesicle is required for normal organogenesis. Development 132:1907 LP-1921.
Kuleshov MV, Jones MR, Rouillard AD, Fernandez NF, Duan Q, Wang Z, Koplev S, Jenkins SL, Jagodnik KM, Lachmann A, et al. 2016. Enrichr: a comprehensive gene set enrichment analysis web server 2016 update. Nucleic Acids Research 44:W90-W97.
Labun K, Montague TG, Krause M, Torres Cleuren YN, Tjeldnes H, Valen E. 2019. CHOPCHOP v3: expanding the CRISPR web toolbox beyond genome editing. Nucleic Acids Research 47:W171-W174.
Lilly AJ, Lacaud G, Kouskoff V. 2017. SOXF transcription factors in cardiovascular development. Semin Cell Dev Biol 63:50-57.
Livak KJ, Schmittgen TD. 2001. Analysis of relative gene expression data using real-time quantitative PCR and the 2(-Delta Delta C(T)) Method. Methods (San Diego, Calif.) 25:402-408.
Livingstone CD, Barton GJ. 1993. Protein sequence alignments: a strategy for the hierarchical analysis of residue conservation. Computer applications in the biosciences : CABIOS 9:745-756.
Long S, Ahmad N, Rebagliati M. 2003. The zebrafish nodal-related gene southpaw is required for visceral and diencephalic left-right asymmetry. Development (Cambridge, England) 130:2303-2316.
Love MI, Huber W, Anders S. 2014. Moderated estimation of fold change and dispersion for RNA-seq data with DESeq2. Genome Biology 15:550.
Lunde K, Belting HG, Driever W. 2004. Zebrafish pou5f1/pou2, Homolog of Mammalian Oct4, Functions in the Endoderm Specification Cascade. Current Biology.
McCurley AT, Callard GV. 2008. Characterization of housekeeping genes in zebrafish: male-female differences and effects of tissue type, developmental stage and chemical treatment. BMC Molecular Biology 9:102.

McDonald Angela CH, Biechele S, Rossant J, Stanford William L. 2014. Sox17-Mediated XEN Cell Conversion Identifies Dynamic Networks Controlling Cell-Fate Decisions in Embryo-Derived Stem Cells. Cell Reports 9:780-793.
Melby AE, Warga RM, Kimmel CB. 1996. Specification of cell fates at the dorsal margin of the zebrafish gastrula. Development 122:2225 LP-2237.
Milewski WM, Duguay SJ, Chan SJ, Steiner DF. 1998. Conservation of PDX-1 Structure, Function, and Expression in Zebrafish*. Endocrinology 139:1440-1449.
Miller AZ, Satchie A, Tannenbaum AP, Nihal A, Thomson JA, Vereide DT. 2018. Expandable Arterial Endothelial Precursors from Human CD34+ Cells Differ in Their Proclivity to Undergo an Endothelial-to-Mesenchymal Transition. Stem Cell Reports 10:73-86.
Mizoguchi T, Verkade H, Heath JK, Kuroiwa A, Kikuchi Y. 2008. Sdf1/Cxcr4 signaling controls the dorsal migration of endodermal cells during zebrafish gastrulation. Development 135:2521-2529.
Montague TG, Gagnon JA, Schier AF. 2018. Conserved regulation of Nodal-mediated left-right patterning in zebrafish and mouse.
Mootha VK, Lindgren CM, Eriksson K-F, Subramanian A, Sihag S, Lehar J, Puigserver P, Carlsson E, Ridderstråle M, Laurila E, et al. 2003. PGC-1α-responsive genes involved in oxidative phosphorylation are coordinately downregulated in human diabetes. Nature Genetics 34:267-273.
Mukherjee S, Chaturvedi P, Rankin SA, Fish MB, Wlizla M, Paraiso KD, MacDonald M, Chen X, Weirauch MT, Blitz IL, et al. 2020. Sox17 and β-catenin co-occupy Wnt-responsive enhancers to govern the endoderm gene regulatory network. eLife 9:e58029-e58029.
Mukherjee S, Luedeke DM, McCoy L, Iwafuchi M, Zorn AM. 2022. SOX transcription factors direct TCF-independent WNT/β-catenin responsive transcription to govern cell fate in human pluripotent stem cells. Cell Reports 40.
Nelson AC, Cutty SJ, Niini M, Stemple DL, Flicek P, Houart C, Bruce AEE, Wardle FC. 2014. Global identification of smad2 and eomesodermin targets in zebrafish identifies a conserved transcriptional network in mesendoderm and a novel role for eomesodermin in repression of ectodermal gene expression. BMC Biology.
Ng CKL, Li NX, Chee S, Prabhakar S, Kolatkar PR, Jauch R. 2012. Deciphering the Sox-Oct partner code by quantitative cooperativity measurements. Nucleic Acids Research 40:4933-4941.
Niakan JHMR, Vokes SA, Rodolfa KT, Sherwood RI, Yamaki M, Dimos JT, Chen AE, Melton DA, McMahon AP, Eggan K. 2010. Sox17 promotes differentiation in mouse embryonic stem cells by directly regulating extraembryonic gene expression and indirectly antagonizing self-renewal. Genes and Development 24:312-326.
Odenthal J, Nüsslein-Volhard C. 1998. fork head domain genes in zebrafish. Development Genes and Evolution 208:245-258.
Palasingam P, Jauch R, Ng CKL, Kolatkar PR. 2009. The structure of Sox17 bound to DNA reveals a conserved bending topology but selective protein interaction platforms. Journal of molecular biology 388:619-630.
Pani L, Overdier DG, Porcella A, Qian X, Lai E, Costa RH. 1992. Hepatocyte Nuclear Factor 3β Contains Two Transcriptional Activation Domains, One of Which Is Novel and Conserved with the Drosophila Fork Head Protein. Molecular and Cellular Biology 12:3723-3732.
Pevny LH, Lovell-Badge R. 1997. Sox genes find their feet. Current opinion in genetics & development 7:338-344.

968 Poulain M. 2006. Zebrafish endoderm formation is regulated by combinatorial Nodal,
969 FGF and BMP signalling. Development.
970 Rebagliati MR, Toyama R, Fricke C, Haffter P, Dawid IB. 1998. Zebrafish Nodal-
971 Related Genes Are Implicated in Axial Patterning and Establishing Left–Right
972 Asymmetry. Developmental Biology 199:261-272.
973 Reim G, Mizoguchi T, Stainier DY, Kikuchi Y, Brand M. 2004. The POU domain
974 protein Spg (Pou2/Oct4) is essential for endoderm formation in cooperation with the
975 HMG domain protein casanova. Developmental Cell.
976 Saba R, Kitajima K, Rainbow L, Engert S, Uemura M, Ishida H, Kokkinopoulos I,
977 Shintani Y, Miyagawa S, Kanai Y, et al. 2019. Endocardium differentiation through
978 Sox17 expression in endocardium precursor cells regulates heart development in
979 mice. Scientific Reports 9:11953.
980 Sarkar A, Hochedlinger K. 2013. The sox family of transcription factors: versatile
981 regulators of stem and progenitor cell fate. Cell stem cell 12:15-30.
982 Saund RS, Kanai-Azuma M, Kanai Y, Kim I, Lucero MT, Saijoh Y. 2012. Gut
983 endoderm is involved in the transfer of left-right asymmetry from the node to the
984 lateral plate mesoderm in the mouse embryo. Development 139:2426-2435.
985 Schneider I, Houston DW, Rebagliati MR, Slusarski DC. 2008. Calcium fluxes in
986 dorsal forerunner cells antagonize β-catenin and alter left-right patterning.
987 Development 135:75-84.
988 Séguin CA, Draper JS, Nagy A, Rossant J. 2008. Establishment of Endoderm
989 Progenitors by SOX Transcription Factor Expression in Human Embryonic Stem
990 Cells. Cell stem cell 3.
991 Sievers F, Higgins DG. 2018. Clustal Omega for making accurate alignments of many
992 protein sequences. Protein Science 27:135-145.
993 Sievers F, Wilm A, Dineen D, Gibson TJ, Karplus K, Li W, Lopez R, McWilliam H,
994 Remmert M, Söding J, et al. 2011. Fast, scalable generation of high-quality protein
995 multiple sequence alignments using Clustal Omega. Molecular Systems Biology
996 7:539.
997 Sinclair AH, Berta P, Palmer MS, Hawkins JR, Griffiths BL, Smith MJ, Foster JW,
998 Frischauf AM, Lovell-Badge R, Goodfellow PN. 1990. A gene from the human sex-
999 determining region encodes a protein with homology to a conserved DNA-binding
1000 motif. Nature 346:240-244.
1001 Sinner D, Rankin S, Lee M, Zorn AM. 2004. Sox17 and beta-catenin cooperate to
1002 regulate the transcription of endodermal genes. Development 131:3069-3080.
1003 Stafford D, White RJ, Kinkel MD, Linville A, Schilling TF, Prince VE. 2006. Retinoids
1004 signal directly to zebrafish endoderm to specify insulin-expressing β-cells.
1005 Development 133:949-956.
1006 Stefanovic S, Abboud N, Desilets S, Nury D, Cowan C, Puceat M. 2009. Interplay of
1007 Oct4 with Sox2 and Sox17: a molecular switch from stem cell pluripotency to
1008 specifying a cardiac fate. J Cell Biol 186:665-673.
1009 Subramanian A, Tamayo P, Mootha VK, Mukherjee S, Ebert BL, Gillette MA,
1010 Paulovich A, Pomeroy SL, Golub TR, Lander ES, et al. 2005. Gene set enrichment
1011 analysis: A knowledge-based approach for interpreting genome-wide expression
1012 profiles. Proceedings of the National Academy of Sciences 102:15545-15550.
1013 Sutherland MJ, Ware SM. 2009. Disorders of left–right asymmetry: Heterotaxy and
1014 situs inversus. American Journal of Medical Genetics Part C: Seminars in Medical
1015 Genetics 151C:307-317.

1016 Sutherland RJ. 1982. The dorsal diencephalic conduction system: A review of the
1017 anatomy and functions of the habenular complex. Neuroscience & Biobehavioral
1018 Reviews 6:1-13.
1019 Talbot CD, Walsh MD, Cutty SJ, Elsayed R, Vlachaki E, Bruce AEE, Wardle FC,
1020 Nelson AC. 2022. Eomes function is conserved between zebrafish and mouse and
1021 controls left-right organiser progenitor gene expression via interlocking feedforward
1022 loops. Frontiers in Cell and Developmental Biology 10.
1023 Tasnim M, Wahlquist P, Hill JT. 2024. Zebrafish: unraveling genetic complexity
1024 through duplicated genes. Dev Genes Evol.
1025 The UniProt C. 2023. UniProt: the Universal Protein Knowledgebase in 2023. Nucleic
1026 Acids Research 51:D523-D531.
1027 Thisse B, Pflumio, S., Fürthauer, M., Loppin, B., Heyer, V., Degrave, A., Woehl, R.,
1028 Lux, A., Steffan, T., Charbonnier, X.Q. and Thisse, C. (2001). 2001. Expression of the
1029 zebrafish genome during embryogenesis (NIH R01 RR15402). In. ZFIN Direct Data
1030 Submission.
1031 Thisse C, Thisse B. 2008. High-resolution in situ hybridization to whole-mount
1032 zebrafish embryos. Nature Protocols 3:59-69.
1033 Traver D, Paw BH, Poss KD, Penberthy WT, Lin S, Zon LI. 2003. Transplantation and
1034 in vivo imaging of multilineage engraftment in zebrafish bloodless mutants. Nature
1035 Immunology 4:1238-1246.
1036 Varadi M, Anyango S, Deshpande M, Nair S, Natassia C, Yordanova G, Yuan D,
1037 Stroe O, Wood G, Laydon A, et al. 2022. AlphaFold Protein Structure Database:
1038 massively expanding the structural coverage of protein-sequence space with high-
1039 accuracy models. Nucleic Acids Research 50:D439-D444.
1040 Viotti M, Niu L, Shi S-H, Hadjantonakis A-K. 2012. Role of the Gut Endoderm in
1041 Relaying Left-Right Patterning in Mice. PLOS Biology 10:e1001276-e1001276.
1042 Voldoire E, Brunet F, Naville M, Volff JN, Galiana D. 2017. Expansion by whole
1043 genome duplication and evolution of the sox gene family in teleost fish. PLoS ONE
1044 12:1-20.
1045 Wagner DE, Weinreb C, Collins ZM, Briggs JA, Megason SG, Klein AM. 2018.
1046 Single-cell mapping of gene expression landscapes and lineage in the zebrafish
1047 embryo. Science 360:981 LP-987.
1048 Warga RM, Kane DA. 2018. Wilson cell origin for kupffer's vesicle in the zebrafish.
1049 Developmental Dynamics 247:1057-1069.
1050 Wegner M. 2010. All purpose Sox: The many roles of Sox proteins in gene
1051 expression. The International Journal of Biochemistry & Cell Biology 42:381-390.
1052 Westerfield M. 2000. The Zebrafish Book. A Guide for The Laboratory Use of
1053 Zebrafish (Danio rerio). Eugene 385.
1054 Wu RS, Lam II, Clay H, Duong DN, Deo RC, Coughlin SR. 2018. A Rapid Method for
1055 Directed Gene Knockout for Screening in G0 Zebrafish. Developmental Cell 46:112-
1056 125.e114.
1057 Yelon D, Horne SA, Stainier DYR. 1999. Restricted Expression of Cardiac Myosin
1058 Genes Reveals Regulated Aspects of Heart Tube Assembly in Zebrafish.
1059 Developmental Biology 214:23-37.
1060 Yuan H, Corbi N, Basilico C, Dailey L. 1995. Developmental-specific activity of the
1061 FGF-4 enhancer requires the synergistic action of Sox2 and Oct-3. Genes and
1062 Development 9:2635-2645.
1063 Zhao J, Lambert G, Meijer AH, Rosa FM. 2013. The transcription factor Vox
1064 represses endoderm development by interacting with x and Pou2. Development.

1065 Zhong TP, Childs S, Leu JP, Fishman MC. 2001. Gridlock signalling pathway fashions
1066 the first embryonic artery. Nature 414:216-220.
1067